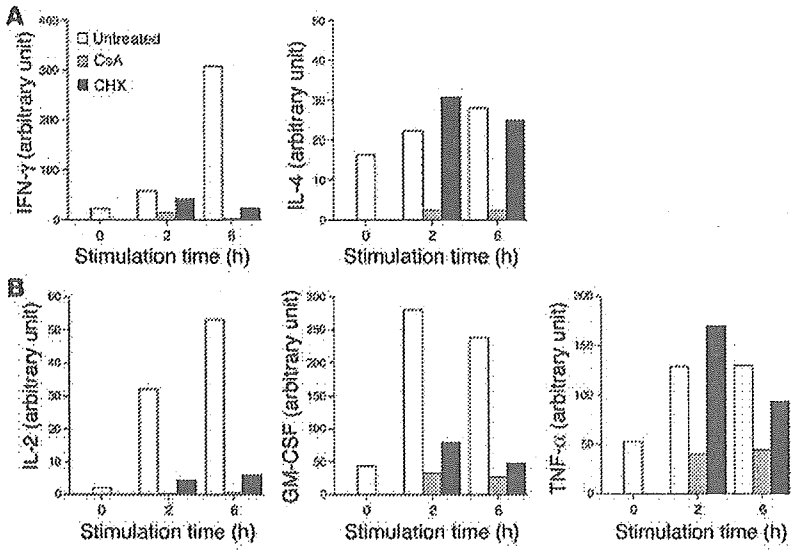

Figure 4
Differential sensitivity to CsA and CHX for transcriptional upregulation of *IFN-γ*, *IL-4*, and other cytokines. (**A**) Sorted NKT cells were pretreated with CsA (1 μg/ml) or with CHX (10 μg/ml) or without either reagent for 10 minutes and were then stimulated with immobilized mAb to CD3 for the indicated periods of time. Total RNA was extracted from each sample and analyzed for the relative amount of transcript of *IFN-γ* or *IL-4*. Data are presented as the amount of transcript in each sample relative to GAPDH. (**B**) Sorted NKT cells were pretreated with CsA (1 μg/ml) or with CHX (10 μg/ml) or without either reagent as shown in **A**. Total RNA was extracted from each sample and was analyzed for the relative amount of transcripts of *IL-2*, *GM-CSF*, or *TNF-α*. Data are presented as the relative amount of transcript in each sample.

tional activation of *IL-4* became evident 30 minutes after TCR stimulation and the transcript accumulated gradually in proportion to the duration of TCR stimulation. This result further confirmed that NKT cells require a longer TCR stimulus for IFN-γ expression.

Transcription of IFN-γ genes depends on c-Rel expression in NKT cells. To further investigate the functional involvement of c-Rel in the transcription of *IFN-γ* gene in NKT cells, we next examined whether forced expression of wild-type c-Rel or of its loss-of-function mutant could affect IFN-γ production by NKT cells. For this, we used bicistronic retroviral vectors expressing c-Rel along with GFP (pMIG/c-Rel) or a c-Rel dominant negative mutant that lacks the C-terminal transactivation domain but retains an intact Rel homology domain of c-Rel protein (pMIG/c-RelΔTA) (21) (Figure 6A). We infected liver-derived mononuclear cells with either retrovirus and stimulated sorted GFP-positive NKT cells with immobilized mAb to CD3 to analyze cytokine production. Retroviral transduction led to expression of GFP in approximately 10% of NKT cells (Figure 6B). Upon stimulation with mAb to CD3, GFP-positive cells from pMIG/c-Rel–infected cultures showed slightly augmented IFN-γ production compared with that of control pMIG-infected cells (Figure 6C). In contrast, GFP-positive cells from pMIG/c-RelΔTA–infected cultures secreted almost no IFN-γ after TCR stimulation (Figure 6C). These results demonstrate that inhibition of c-Rel function, via the introduction of a mutant form of c-Rel, abolishes IFN-γ production and that functional c-Rel is important for effective production of IFN-γ in activated NKT cells.

Discussion

In this study, we investigated the molecular mechanism for differential production of IFN-γ and IL-4 by activated NKT cells through a comparative analysis using the prototypic NKT cell ligands αGC and OCH. Treatment with αGC induced expression of both IFN-γ and IL-4 simultaneously, but OCH induced selective expression of IL-4 by NKT cells. Furthermore, we demonstrated that the CD1d-associated glycolipids with various lipid chain lengths showed different half-lives for NKT cell stimulation when applied in an endosome/lysosome-independent manner and induced the differential cytokine production by NKT cells in a lipid length–dependent manner. Accordingly, we demonstrated that IFN-γ production by NKT cells required longer TCR stimulation than did IL-4 production and depended on de novo protein synthesis. An NF-κB family transcription factor gene, the *c-Rel* gene, was inducibly transcribed in αGC-stimulated but not in OCH-stimulated NKT cells. Retroviral transduction of a loss-of-function mutant of c-Rel revealed the functional involvement of c-Rel in IFN-γ production by ligand-activated NKT cells. These results have provided a new interpretation of NKT cell activation — that the duration of TCR stimulation is critically influenced by the stability of each glycolipid ligand on CD1d molecules, which leads to the differential cytokine production by NKT cells.

We have previously demonstrated that administration of OCH consistently suppresses the development of EAE by inducing a Th2 bias in autoimmune T cells and that this Th2 shift is probably mediated by selective IL-4 production by NKT cells in vivo (9). Here we directly evaluated the cytokine profile of OCH-stimulated NKT cells using quantitative PCR analysis. Consistent with the previous assumption, NKT cells stimulated with OCH induced rapid production of IL-4 but led to only marginal induction of IFN-γ, confirming the presumed mechanism for the effect of OCH on EAE and CIA. As the "fold induction" of *IFN-γ* transcript after 1.5 hours of stimulation with αGC in microarray analysis was relatively low (fivefold for liver NKT cells and fourfold for spleen NKT cells) compared with the in vivo data, there are several possibilities to explain these results. First, quiescent transcripts of *IFN-γ* pre-existing in resting Vα14-invariant NKT cells (22) may raise the baseline of signal intensity in samples from untreated animals, resulting in a relative decrease in "fold induction" after glycolipid treatment. Second, detection of *IFN-γ* transcription in αGC-stimulated NKT cells might not be optimal, as injection of αGC induced a rapid elevation in IL-4 with the peak value at 2 hours and a delayed and prolonged elevation in IFN-γ in B6 mice (9). Third, αGC treatment significantly induces transcription of *CD154* (18.0-fold for αGC vs. 5.4-fold for OCH; data not shown), whose promoter has a functional NF-AT binding site and CD28 responsive element (CD28RE) (23, 24). Thus, augmented CD40/CD154 interaction may induce IL-12 expression by APCs, resulting in additional IFN-γ production (25). Finally, NKT cells are not necessarily the only source of IFN-γ after in vivo stimulation with αGC. The "serial" production of IFN-γ by NKT cells and NK cells has been demonstrated (6, 26). In particular, a C-glycoside analog of αGC has

Table 2
Differential gene expression patterns in αGC-treated and OCH-treated murine NKT cells

		Liver CD3+NK1.1+							Spleen CD3+NK1.1+						
		Untreated	αGC			OCH			Untreated	αGC			OCH		
Common name	GenBank		1.5 h		12 h	1.5 h		12 h		1.5 h		12 h	1.5 h		12 h
IFN-γ	K00083	1.0 P	5.0	P	0.3 P	1.2	P	0.1 P	1.0 P	4.0	P	2.3 P	0.7	P	1.0 P
IL-2	m16762	1.0 A	391.4	P	1.2 A	12.3	P	1.3 A	1.0 A	23.4	P	0.2 A	1.0	A	0.3 A
IL-2	K02292	1.0 A	129.6	P	0.6 A	32.8	A	1.1 A	1.0 A	16.1	A	0.7 A	10.7	A	1.5 A
GM-CSF	X03020	1.0 P	38.0	P	0.4 A	4.1	P	0.1 A	1.0 A	15.7	P	1.4 A	2.7	A	2.1 A
IL-4	X03532	1.0 P	276.8	P	2.5 P	47.3	P	0.2 A	1.0 A	364.9	P	35.1 P	38.8	P	4.7 P
IL-4	M25892	1.0 P	38.2	P	0.2 P	7.7	P	0.1 A	1.0 P	69.6	P	7.6 P	9.1	P	1.1 P
IL-4	X03532	1.0 A	34.8	P	3.9 A	9.4	A	1.9 A	1.0 A	2.2	A	4.2 A	1.1	A	0.7 A
IL-13	M23504	1.0 A	993.0	P	1.4 A	56.1	P	1.8 A	1.0 A	140.7	P	12.3 A	19.1	A	2.3 A
TNF-α	D84196	1.0 P	30.8	P	2.1 P	1.7	P	1.2 P	1.0 P	16.5	P	2.5 P	1.8	P	2.6 P
Lymphotoxin A	M16819	1.0 P	6.9	P	0.2 A	1.4	P	0.1 A	1.0 P	2.5	P	1.7 P	1.2	P	0.9 P
IL-1α	M14639	1.0 P	25.1	P	5.6 P	3.1	P	4.4 P	1.0 P	6.7	P	5.8 P	1.1	P	2.7 P
IL-1β	M15131	1.0 P	8.0	P	9.8 P	1.3	P	7.9 P	1.0 P	3.3	P	2.2 P	0.6	P	1.5 P
*IL-1*RA	L32838	1.0 P	10.9	P	15.2 P	1.1	A	11.3 P	1.0 P	5.3	P	28.0 P	0.9	P	23.4 P
IL-3	K01668	1.0 A	33.2	P	2.6 A	4.7	A	1.2 A	1.0 A	4.0	A	1.1 A	1.4	A	1.7 A
IL-6	X54542	1.0 A	34.8	P	16.5 P	8.8	P	10.7 P	1.0 A	19.1	P	17.8 P	1.8	A	12.2 A

Real-time PCR analyses were conducted for *IFN-γ* and *IL-4* as well as for other selected cytokine genes listed in Figure 4 (data not shown) to confirm the correlation with those obtained from microarray analysis. Each probe was assigned a "call" of present (P; expressed) or "absent" (A; not expressed) using the Affymetrix decision matrix. GenBank, GenBank accession number; *IL-1*RA, *IL-1* receptor antagonist.

recently been shown to induce Th1-type activity superior to that induced by αGC, and IL-12 is indispensable for the Th1-skewing effect of the analog (27), indicating the importance of IL-12 in augmenting IFN-γ production in vivo (14, 28). Interestingly, the C-glycoside analog induces production of IFN-γ and IL-4 by NKT cells less strongly than does αGC at 2 hours after in vivo administration. Given that αGC and C-glycoside analog have the same structure for their lipid tails, they might be expected to have comparable affinity for CD1d molecules, and the slightly "twirled" α-anomeric galactose moiety between C-glycoside and O-glycoside may modulate the agonistic effect of these glycolipids. Furthermore, the C-glycoside is more resistant to hydrolysis in vivo and may have an advantage for effective production of IL-12 by APCs. In fact, OCH induces marginal IL-12 production after in vivo administration (data not shown), which makes it unable to induce IFN-γ production by various cells. Therefore, the beneficial feature of OCH as an immunomodulator is that it does not trigger production of IFN-γ in vivo.

As described previously, NKT cells recognize glycolipid antigens in the context of the nonpolymorphic MHC class I-like molecule CD1d (4). Crystal structure analysis revealed that the mouse CD1d molecule has a narrow and deep binding groove with extremely hydrophobic pockets, A′ and F′ (29). Thus the two aliphatic hydrocarbon chains would be captured by this binding groove of CD1d and the more hydrophilic galactose moiety of αGC or OCH would be presented to TCR on NKT cells. As OCH is an analog of αGC with a truncated sphingosine chain, it could be predicted that truncation of the hydrocarbon chain would make it more unstable on CD1d, which might then affect the duration of TCR stimulation on NKT cells. We demonstrated in this study that OCH detached from the CD1d molecule more rapidly than did αGC after a short-term pulse in which the glycolipids were segregated from the endosomal/lysosomal pathway. Accordingly, we showed that the initiation of IFN-γ production by NKT cells required more prolonged TCR stimulation than was required for IL-4 production. Methods such as surface plasmon resonance were not appropriate for direct assessment of the interaction between glycolipids and CD1d, possibly because of unpredictable micelle formation and the poor solubility of glycolipids in aqueous solvents (30). The half-life of the interaction of glycolipids and CD1d was reported to be less than 1 minute by surface plasmon resonance (31), contradicting functional assays suggesting a much longer half-life. Therefore, we applied a biological assay to evaluate the stability of these glycolipids on CD1d molecules, as described previously (13).

The characteristics of OCH are somewhat analogous to those of an altered peptide ligand (APL) that has been shown to induce a subset of functional responses observed in intact peptide and, in some cases, induce production of selected cytokines by T cells (32–34). Thus, OCH and possibly other αGC derivatives could be called "altered glycolipid ligands" (AGLs). Although the biological effects of APLs and AGLs could mediate a series of similar molecular events in target cells, it should be noted that APLs and AGLs differ in their "conceptual features." That is, APLs are usually altered in their amino acid residues to modify their affinity for TCRs, whereas AGLs have truncation of their hydrocarbon chain responsible for CD1d anchoring. This paper has highlighted the duration of NKT cell stimulation by CD1d-associated glycolipids as being a critical factor for determining the nature of AGLs for selective induction of cytokine production by NKT cells.

Given that IL-4 secretion consistently precedes IFN-γ production by NKT cells after TCR ligation, we speculated there were critical differences in the upstream transcriptional requirements for the *IFN-γ* and *IL-4* genes in NKT cells. In support of this speculation, CHX treatment specifically inhibited the transcription of *IFN-γ* but not that of *IL-4*. In contrast, transcription of both cytokines was abolished by CsA treatment, indicating that TCR-mediated activation of NF-AT is essential for the production of both cytokines. TCR signal–induced NF-AT activation occurs promptly corresponding to calcium influx (35). Meanwhile, the protein expression of specific

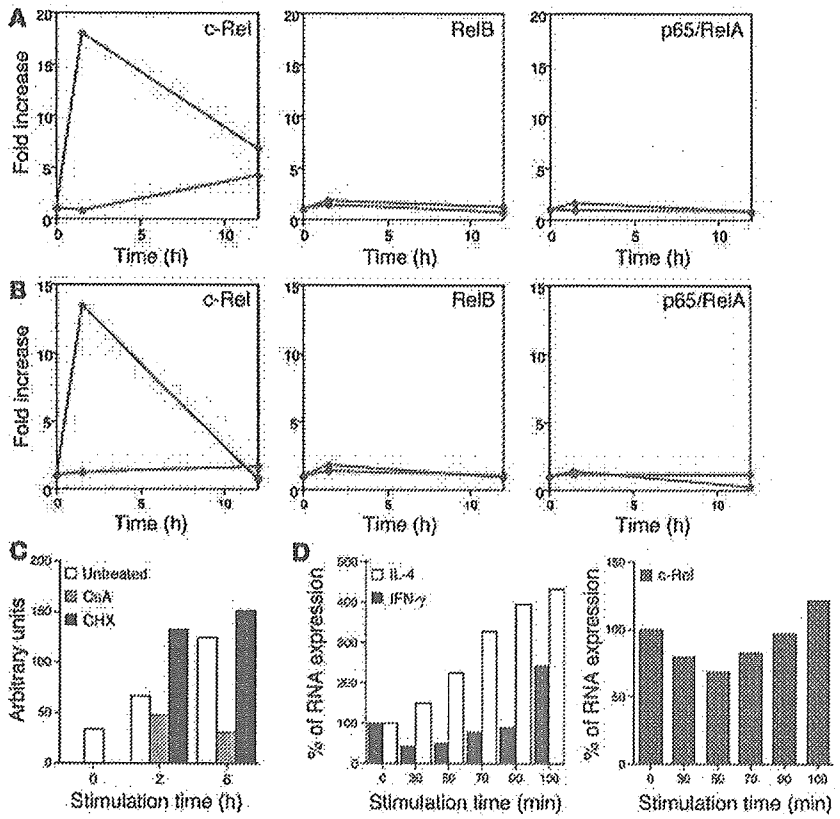

Figure 5
Induction of NF-κB family members in activated NKT cells. (**A**) Plotted values represent data of Affymetrix microarray analysis for the indicated genes. The αGC-stimulated (red lines) or OCH-stimulated (green lines) cells as well as unstimulated liver NKT cells were analyzed at the same time points and the data are presented as the relative value for stimulated NKT cells when the value in NKT cells derived from untreated animals was defined as 1. (**B**) Real-time PCR analysis for the same genes as in **A**. Data are presented as described in Figure 4. (**C**) Sorted liver NKT cells were pretreated with CsA or CHX and were stimulated with immobilized mAb to CD3, and comparative values of c-Rel transcripts relative to GAPDH were determined. (**D**) Sorted liver NKT cells were stimulated with immobilized mAb to CD3 for the indicated periods of time and then were cultured without stimulation for up to a total of 120 minutes after the initial stimulation. Total RNA was extracted from each sample and analyzed for relative amounts of transcripts of *IFN-γ* or *IL-4* (left), or *c-Rel* (right). The amount of RNA derived from unstimulated NKT cells was defined as 100%.

transcription factors takes more time to accomplish. The requirement for prolonged TCR stimulation for initiation of *IFN-γ* transcription may be due to its dependency on specific gene expression.

Recently, Matsuda et al. have shown using cytokine reporter mice that Vα14-invariant NKT cells express cytokine transcripts in the resting state, but express protein only after stimulation (22). We obtained a similar result with our microarray analysis, in that many cytokine transcripts including *IFN-γ* and *IL-4* were detectable in unstimulated NKT cells derived from liver or spleen, because most of them were assigned a "call" of "present" by the Affymetrix decision matrix, which means they were significantly expressed. The mechanism of translation of pre-existing cytokine transcripts after activation of NKT cells remains to be investigated.

Through microarray analysis and real-time PCR, we next identified a member of the NF-κB family of transcription factors, c-Rel, as being a protein rapidly expressed after αGC treatment and possibly responsible for the transcription of *IFN-γ*. Treatment with αGC selectively upregulated *c-Rel* transcription 1.5 hours after stimulation of NKT cells in vivo. OCH treatment, however, showed no induction of *c-Rel* transcription. Although *c-Rel* is transcriptionally upregulated after TCR stimulation of T cells (36), transcription of other NF-κB family members such as *p65/RelA*, *RelB*, *NF-κB1*, and *NF-κB2* was unchanged (data not shown). CsA treatment inhibited c-Rel transcription, but CHX did not, indicating that inducible transcription of c-Rel was directly controlled by TCR signal–mediated activation of NF-AT, which is consistent with a previous report (19). Although the pre-existing NF-κB proteins in general provide a means of rapidly altering cellular responses by inducing the destruction of IκB in order to enable NF-κB to be free for nuclear translocation and DNA binding, most of the nuclear c-Rel induced after T cell stimulation has been shown to be derived from newly translated c-Rel proteins. In contrast, pre-existing c-Rel scarcely translocates to the nucleus at all (36), indicating that the nuclear induction of c-Rel in T lymphocyte requires ongoing protein synthesis. The retrovirally transduced loss-of-function mutant c-Rel (c-RelΔTA) significantly inhibited transcription of *IFN-γ* genes, indicating the crucial role of c-Rel in their transcription after activation of NKT cells. Although it is possible that the Rel domain of the dominant negative mutant may affect a number of NF-κB dimers, it is unlikely, because IFN-γ production by stimulated NKT cells were CHX sensitive and other NK-κB members were not induced after stimulation in the microarray analysis. Retroviral transduction of wild-type c-Rel into NKT cells resulted in slightly augmented expression of IFN-γ after stimulation. Induction of endogenous c-Rel after in vitro stimulation might reduce the effect of retrovirally introduced c-Rel protein.

Whereas c-Rel has been associated with the functions of various cell types, its role in the immune system was first demonstrated in its involvement in *IL-2* transcription (37), in which it possibly induced chromatin remodeling of the promoter (38). Recently, the promoters for the genes encoding *IL-3*, *IL-5*, *IL-6*, *TNF-α*, *GM-CSF*, and *IFN-γ* were shown to contain κB sites or the κB-related CD28RE. Gene targeting of *c-Rel* in mice revealed that *c-Rel*–deficient T cells have a defect in the production of IL-2, IL-3, IL-5, GM-CSF, TNF-α, and IFN-γ, although expression of some of the cytokines was rescued by the addition of exogenous IL-2 (39, 40). Regarding the involvement of c-Rel in IFN-γ production, the c-Rel inhibitor pentoxyfylline (41) selectively suppresses Th1 cytokine production and EAE induction (42), and transgenic mice expressing the *trans*-dominant form of IκBα have a defect in IFN-γ production and the Th1 response (43). Recently, an elegant study using *c-Rel*–deficient mice revealed *c-Rel* has crucial roles in IFN-γ production by activated T cells and conse-

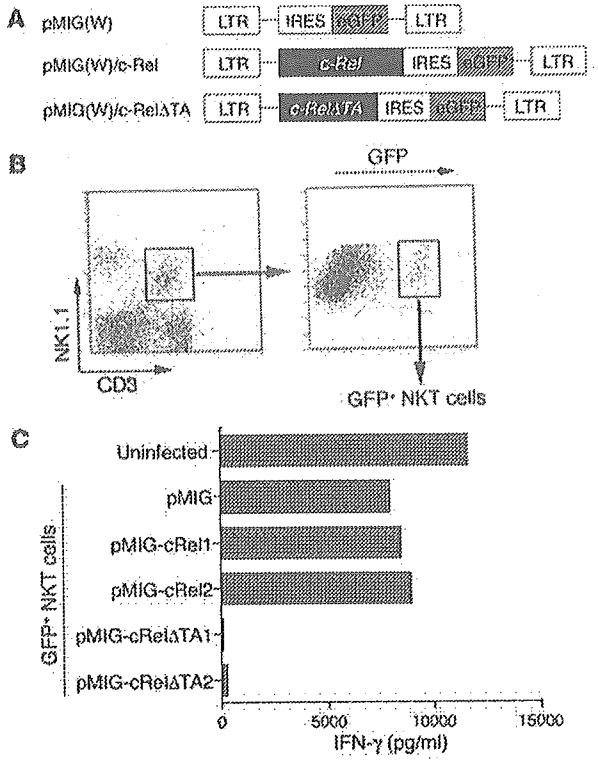

Figure 6
Cytokine production after retroviral transduction of c-Rel or c-RelΔTA into NKT cells. (**A**) DNA fragments encoding wild-type c-Rel or its mutant were cloned into the pMIG(W) bicistronic retrovirus vector. The mutant form of c-Rel (c-RelΔTA) lacks the transactivation domain of the c-Rel protein. LTR, long terminal repeat; IRES, internal ribosome entry site; eGFP, enhanced GFP. (**B**) Flow cytometric identification of cells transfected with the viral vector. Among the NK1.1$^+$CD3$^+$ liver NKT cells identified in the left panel, approximately 10% were GFP positive. The GFP-positive NKT cells were sorted for further analysis. (**C**) IFN-γ production by NKT cells transfected with c-Rel or its dominant negative mutant. The CD3$^+$NK1.1$^+$ NKT cells infected with the viruses were isolated based on their expression of GFP and were stimulated with immobilized mAb to CD3. For transduction of c-Rel or c-RelΔTA into NKT cells, two independent clones of each retroviral vector were used. The level of IFN-γ in the supernatants was measured by ELISA.

quent Th1 development by affecting the cellular functions of both T cells and APCs (20). Thus, the critical involvement of c-Rel for IFN-γ production in NKT cells is consistent with these findings.

Our results indicate that rapid calcium influx and subsequent NF-AT activation is essential for IFN-γ production by activated NKT cells and that c-Rel plays a crucial role in IFN-γ production as well. NF-AT shows quick and sensitive nucleocytoplasmic shuttling after TCR activation (35). Feske et al. demonstrated that the pattern of cytokine production by T cells was determined by the duration of nuclear residence of NF-AT (44) and that sustained NF-AT signaling promoted IFN-γ expression in CD4$^+$ T cells (45). Considering the structural feature of αGC with longer lipid chain, sustained stimulation by αGC induces long-lasting calcium influx, resulting in sustained nuclear residence of NF-AT, and c-Rel protein synthesis, which enables NKT cells to produce IFN-γ. In contrast, the rather sporadic stimulation by OCH induces short-lived nuclear residence of NF-AT, followed by marginal c-Rel expression, which leaves NKT cells unable to produce IFN-γ (Figure 7). Thus, the kinetic and quantitative differences between αGC and OCH in the induction of transcription factors, such as NF-AT and c-Rel, determine the pattern of cytokine production by NKT cells. As CD1d molecules are nonpolymorphic and are remarkably well conserved among the species, the preferential induction of IL-4 production through NKT activa-

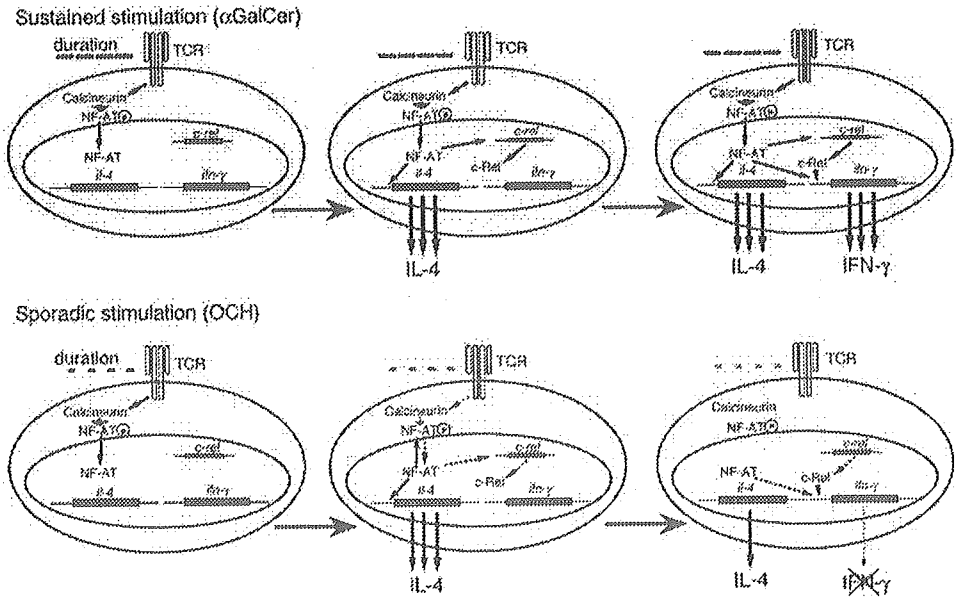

Figure 7
A model for the differential expression of IFN-γ and IL-4 after treatment of NKT cells with αGC or OCH. See text for details.

tion and subsequent Th2 polarization suggest that OCH may be an attractive therapeutic reagent to use for Th1-mediated autoimmune diseases such as multiple sclerosis and rheumatoid arthritis.

Acknowledgments

We thank Kyoko Hayakawa and Sebastian Joyce for providing the cell lines; Thomas Grundström for providing the c-Rel plasmid; and Luk Van Parijs for providing the retroviral vectors and packaging vector. We also thank Miho Mizuno and Chiharu Tomi for excellent technical assistance; and Yuki Kikai for cell sorting. We are grateful to John Ludvic Croxford for critical reading of the manuscript. This work was supported by the Organization for Pharmaceutical Safety and Research, Grant-in-Aid for Scientific Research (B) 14370169 from Japan Society for the Promotion of Science, Mochida Memorial Foundation, and Uehara Memorial Foundation.

Received for publication December 18, 2003, and accepted in revised form April 6, 2004.

Address correspondence to: Sachiko Miyake, Department of Immunology, National Institute of Neuroscience, NCNP, 4-1-1 Ogawahigashi, Kodaira, Tokyo 187-8502, Japan. Phone: 81-42-341-2711; Fax: 81-42-346-1753; E-mail: miyake@ncnp.go.jp.

1. Kronenberg, M., and Gapin, L. 2002. The unconventional lifestyle of NKT cells. *Nat. Rev. Immunol.* **2**:557–568.
2. Taniguchi, M., Harada, M., Kojo, S., Nakayama, T., and Wakao, H. 2003. The regulatory role of Vα14 NKT cells in innate and acquired immune response. *Annu. Rev. Immunol.* **21**:483–513.
3. Brossay, L., et al. 1998. CD1d-mediated recognition of an α-galactosylceramide by natural killer T cells is highly conserved through mammalian evolution. *J. Exp. Med.* **188**:1521–1528.
4. Kawano, T., et al. 1997. CD1d-restricted and TCR-mediated activation of vα14 NKT cells by glycosylceramides. *Science.* **278**:1626–1629.
5. Spada, F.M., et al. 1998. CD1d-restricted recognition of synthetic glycolipid antigens by human natural killer T cells. *J. Exp. Med.* **188**:1529–1534.
6. Carnaud, C., et al. 1999. Cross-talk between cells of the innate immune system: NKT cells rapidly activate NK cells. *J. Immunol.* **163**:4647–4650.
7. Fujii, S.I., Shimizu, K., Smith, C., Bonifaz, L., and Steinman, R.M. 2003. Activation of natural killer T cells by α-galactosylceramide rapidly induces the full maturation of dendritic cells in vivo and thereby acts as an adjuvant for combined CD4 and CD8 T cell immunity to a coadministered protein. *J. Exp. Med.* **198**:267–279.
8. Chiba, A., et al. 2004. Suppression of collagen-induced arthritis by natural killer T cell activation with OCH, a sphingosine-truncated analog of α-galactosylceramide. *Arthritis Rheum.* **50**:305–313.
9. Miyamoto, K., Miyake, S., and Yamamura, T. 2001. A synthetic glycolipid prevents autoimmune encephalomyelitis by inducing TH2 bias of natural killer T cells. *Nature.* **413**:531–534.
10. Burdin, N., et al. 1998. Selective ability of mouse CD1 to present glycolipids: α-galactosylceramide specifically stimulates Vα 14+ NK T lymphocytes. *J. Immunol.* **161**:3271–3281.
11. De Silva, A.D., et al. 2002. Lipid protein interactions: the assembly of CD1d1 with cellular phospholipids occurs in the endoplasmic reticulum. *J. Immunol.* **168**:723–733.
12. Antonsson, A., Hughes, K., Edin, S., and Grundstrom, T. 2003. Regulation of c-Rel nuclear localization by binding of Ca2+/calmodulin. *Mol. Cell. Biol.* **23**:1418–1427.
13. Moody, D.B., et al. 2002. Lipid length controls antigen entry into endosomal and nonendosomal pathways for CD1b presentation. *Nat. Immunol.* **3**:435–442.
14. Fujii, S., Shimizu, K., Kronenberg, M., and Steinman, R.M. 2002. Prolonged IFN-γ-producing NKT response induced with α-galactosylceramide-loaded DCs. *Nat. Immunol.* **3**:867–874.
15. Akbari, O., et al. 2003. Essential role of NKT cells producing IL-4 and IL-13 in the development of allergen-induced airway hyperreactivity. *Nat. Med.* **31**:31.
16. Heller, F., Fuss, I.J., Nieuwenhuis, E.E., Blumberg, R.S., and Strober, W. 2002. Oxazolone colitis, a Th2 colitis model resembling ulcerative colitis, is mediated by IL-13-producing NK-T cells. *Immunity.* **17**:629–638.
17. Leite-de-Moraes, M.C., et al. 2002. Ligand-activated natural killer T lymphocytes promptly produce IL-3 and GM-CSF in vivo: relevance to peripheral myeloid recruitment. *Eur. J. Immunol.* **32**:1897–1904.
18. Chen, H., Huang, H., and Paul, W.E. 1997. NK1.1+ CD4+ T cells lose NK1.1 expression upon in vitro activation. *J. Immunol.* **158**:5112–5119.
19. Venkataraman, L., Burakoff, S.J., and Sen, R. 1995. FK506 inhibits antigen receptor-mediated induction of c-rel in B and T lymphoid cells. *J. Exp. Med.* **181**:1091–1099.
20. Hilliard, B.A., et al. 2002. Critical roles of c-Rel in autoimmune inflammation and helper T cell differentiation. *J. Clin. Invest.* **110**:843–850. doi:10.1172/JCI200215254.
21. Carrasco, D., et al. 1998. Multiple hemopoietic defects and lymphoid hyperplasia in mice lacking the transcriptional activation domain of the c-Rel protein. *J. Exp. Med.* **187**:973–984.
22. Matsuda, J.L., et al. 2003. Mouse Vα14i natural killer T cells are resistant to cytokine polarization in vivo. *Proc. Natl. Acad. Sci. U. S. A.* **100**:8395–8400.
23. Tsytsykova, A.V., Tsitsikov, E.N., and Geha, R.S. 1996. The CD40L promoter contains nuclear factor of activated T cells-binding motifs which require AP-1 binding for activation of transcription. *J. Biol. Chem.* **271**:3763–3770.
24. Parra, E., Mustelin, T., Dohlsten, M., and Mercola, D. 2001. Identification of a CD28 response element in the CD40 ligand promoter. *J. Immunol.* **166**:2437–2443.
25. Kitamura, H., et al. 1999. The natural killer T (NKT) cell ligand α-galactosylceramide demonstrates its immunopotentiating effect by inducing interleukin (IL)-12 production by dendritic cells and IL-12 receptor expression on NKT cells. *J. Exp. Med.* **189**:1121–1128.
26. Smyth, M.J., et al. 2002. Sequential production of interferon-γ by NK1.1+ T cells and natural killer cells is essential for the antimetastatic effect of α-galactosylceramide. *Blood.* **99**:1259–1266.
27. Schmieg, J., Yang, G., Franck, R.W., and Tsuji, M. 2003. Superior protection against malaria and melanoma metastases by a C-glycoside analogue of the natural killer T cell ligand α-galactosylceramide. *J. Exp. Med.* **198**:1631–1641.
28. Brigl, M., Bry, L., Kent, S.C., Gumperz, J.E., and Brenner, M.B. 2003. Mechanism of CD1d-restricted natural killer T cell activation during microbial infection. *Nat. Immunol.* **4**:1230–1237.
29. Zeng, Z., et al. 1997. Crystal structure of mouse CD1: An MHC-like fold with a large hydrophobic binding groove. *Science.* **277**:339–345.
30. Cantu, C., 3rd, Benlagha, K., Savage, P.B., Bendelac, A., and Teyton, L. 2003. The paradox of immune molecular recognition of α-galactosylceramide: low affinity, low specificity for CD1d, high affinity for αβ TCRs. *J. Immunol.* **170**:4673–4682.
31. Benlagha, K., Weiss, A., Beavis, A., Teyton, L., and Bendelac, A. 2000. In vivo identification of glycolipid antigen-specific T cells using fluorescent CD1d tetramers. *J. Exp. Med.* **191**:1895–1903.
32. Evavold, B.D., and Allen, P.M. 1991. Separation of IL-4 production from Th cell proliferation by an altered T cell receptor ligand. *Science.* **252**:1308–1310.
33. Chaturvedi, P., Yu, Q., Southwood, S., Sette, A., and Singh, B. 1996. Peptide analogs with different affinities for MHC alter the cytokine profile of T helper cells. *Int. Immunol.* **8**:745–755.
34. Boutin, Y., Leitenberg, D., Tao, X., and Bottomly, K. 1997. Distinct biochemical signals characterize agonist- and altered peptide ligand-induced differentiation of naive CD4+ T cells into Th1 and Th2 subsets. *J. Immunol.* **159**:5802–5809.
35. Zhu, J., and McKeon, F. 2000. Nucleocytoplasmic shuttling and the control of NF-AT signaling. *Cell. Mol. Life Sci.* **57**:411–420.
36. Venkataraman, L., Wang, W., and Sen, R. 1996. Differential regulation of c-Rel translocation in activated B and T cells. *J. Immunol.* **157**:1149–1155.
37. Ghosh, P., Tan, T.H., Rice, N.R., Sica, A., and Young, H.A. 1993. The interleukin 2 CD28-responsive complex contains at least three members of the NF κ B family: c-Rel, p50, and p65. *Proc. Natl. Acad. Sci. U. S. A.* **90**:1696–1700.
38. Rao, S., Gerondakis, S., Woltring, D., and Shannon, M.F. 2003. c-Rel Is required for chromatin remodeling across the IL-2 gene promoter. *J. Immunol.* **170**:3724–3731.
39. Gerondakis, S., et al. 1996. Rel-deficient T cells exhibit defects in production of interleukin 3 and granulocyte-macrophage colony-stimulating factor. *Proc. Natl. Acad. Sci. U. S. A.* **93**:3405–3409.
40. Kontgen, F., et al. 1995. Mice lacking the c-rel proto-oncogene exhibit defects in lymphocyte proliferation, humoral immunity, and interleukin-2 expression. *Genes Dev.* **9**:1965–1977.
41. Wang, W., Tam, W.F., Hughes, C.C., Rath, S., and Sen, R. 1997. c-Rel is a target of pentoxifylline-mediated inhibition of T lymphocyte activation. *Immunity.* **6**:165–174.
42. Rott, O., Cash, E., and Fleischer, B. 1993. Phosphodiesterase inhibitor pentoxifylline, a selective suppressor of T helper type 1- but not type 2-associated lymphokine production, prevents induction of experimental autoimmune encephalomyelitis in Lewis rats. *Eur. J. Immunol.* **23**:1745–1751.
43. Aronica, M.A., et al. 1999. Preferential role for NF-κ B/Rel signaling in the type 1 but not type 2 T cell-dependent immune response in vivo. *J. Immunol.* **163**:5116–5124.
44. Feske, S., Draeger, R., Peter, H.H., Eichmann, K., and Rao, A. 2000. The duration of nuclear residence of NFAT determines the pattern of cytokine expression in human SCID T cells. *J. Immunol.* **165**:297–305.
45. Porter, C.M., and Clipstone, N.A. 2002. Sustained NFAT signaling promotes a Th1-like pattern of gene expression in primary murine CD4+ T cells. *J. Immunol.* **168**:4936–4945.

American Journal of Pathology, Vol. 165, No. 2, August 2004

The 14-3-3 Protein ϵ Isoform Expressed in Reactive Astrocytes in Demyelinating Lesions of Multiple Sclerosis Binds to Vimentin and Glial Fibrillary Acidic Protein in Cultured Human Astrocytes

Jun-ichi Satoh,* Takashi Yamamura,* and Kunimasa Arima†

From the Department of Immunology, National Institute of Neuroscience, and the Department of Neuropathology,† National Center Hospital for Mental, Nervous, and Muscular Disorders, National Center of Neurology and Psychiatry, Tokyo, Japan*

The 14-3-3 protein family consists of acidic 30-kd proteins expressed at high levels in neurons of the central nervous system. Seven isoforms form a dimeric complex that acts as a molecular chaperone that interacts with key signaling components. Recent studies indicated that the 14-3-3 protein identified in the cerebrospinal fluid of various neurological diseases including multiple sclerosis (MS) is a marker for extensive brain destruction. However, it remains unknown whether the 14-3-3 protein plays an active role in the pathological process of MS. To investigate the differential expression of seven 14-3-3 isoforms in MS lesions, brain tissues of four progressive cases were immunolabeled with a panel of isoform-specific antibodies. Reactive astrocytes in chronic demyelinating lesions intensely expressed β, ϵ, ζ, η, and σ isoforms, among which the ϵ isoform is a highly specific marker for reactive astrocytes. Furthermore, protein overlay, mass spectrometry, immunoprecipitation, and double-immunolabeling analysis showed that the 14-3-3 protein interacts with both vimentin and glial fibrillary acidic protein in cultured human astrocytes. These results suggest that the 14-3-3 protein plays an organizing role in the intermediate filament network in reactive astrocytes at the site of demyelinating lesions in MS. *(Am J Pathol 2004, 165:577–592)*

The 14-3-3 protein family consists of evolutionarily conserved, acidic 30-kd proteins originally identified by two dimensional analysis of brain protein extract.[1–4] Seven isoforms of the 14-3-3 protein named β, γ, ϵ, ζ, η, θ (also termed as τ), and σ have been identified in eukaryotic cells. Although the 14-3-3 protein is widely distributed in neural and nonneural tissues, it is expressed most abundantly in neurons in the central nervous system (CNS), where it represents 1% of total cytosolic proteins.[4–7] A homodimeric or heterodimeric complex, which is composed of the same or distinct isoforms of the 14-3-3 protein, constitutes a large cup-like structure with two ligand-binding sites in its groove. The dimeric complex acts as a novel molecular chaperone that interacts with key molecules involved in cell differentiation, proliferation, transformation, and apoptosis.[1–4] It regulates the function of target proteins by restricting their subcellular location, bridging them to modulate catalytic activity, and protecting them from dephosphorylation or proteolysis.[1–4,8–10] In general, the 14-3-3 protein binds to phosphoserine-containing motifs of the ligands such as RSXpSXP and RXY/FXpSXP in a sequence-specific manner.[1–3,10] More than 100 proteins have been identified as being 14-3-3 binding partners, including a range of intracellular signaling regulators such as Raf, BAD, protein kinase C (PKC), phophatidylinositol 3-kinase (PI3K), and cdc25 phosphatase.[1–4,8–10] Binding of the 14-3-3 protein to Raf is indispensable for Raf kinase activity in the Ras/MAPK signaling pathway, whereas 14-3-3 binding to the mitochondrial Bcl-2 family member BAD, when phosphorylated by a serine/threonine kinase Akt, inhibits apoptosis.[1–4] In addition to the phosphorylation-dependent interaction, the 14-3-3 protein can interact with a set of target proteins in a phosphorylation-independent manner.[10–12] The ϵ isoform binds to p190RhoGEF via a phosphoserine-independent interaction.[11]

Previous studies indicated that the 14-3-3 protein has isoform-specific and nonredundant functions.[1–4] Synaptic transmission and associative learning are impaired in

Supported by the Grant-in-Aid for Scientific Research (B2-15390280 and PA007-16017320); the Ministry of Education, Science, Sports, and Culture; and the Organization for Pharmaceutical Safety and Research, Kiko, Japan.

Accepted for publication April 22, 2004.

During submission of the present manuscript, an immunohistochemical study (Kawamoto Y, Akiguchi I, Kovács GG, Flicker H, Budka H: Increased 14-3-3 immunoreactivity in glial elements in patients with multiple sclerosis. Acta Neuropathol 2004, 107:137–143) has been published. This study showed that the 14-3-3 protein is expressed strongly in both astrocytes and oligodendrocytes in MS brains using an anti-14-3-3 protein antibody broadly reactive against all isoforms (H-8, sc-1657; Santa Cruz Biotechnology).

Supplemental information can be found on *http://www.amjpathol.org*.

Address reprint requests to Dr. Jun-ichi Satoh, Department of Immunology, National Institute of Neuroscience, NCNP, 4-1-1 Ogawahigashi, Kodaira, Tokyo 187-8502, Japan. E-mail: satoj@ncnp.go.jp.

Drosophila mutants lacking the ζ protein.[13] The 14-3-3 isoforms have distinct affinities for their target proteins. A preferential interaction is observed between PKCθ and the human 14-3-3θ isoform in T cells,[14] IGF1-receptor, IRS1, and ϵ isoform,[15] the apoptosis-inhibitor A20 and the human β and η isoforms,[16] and glucocorticoid receptor and the human η isoform.[17] The human β and ζ isoforms and not γ or ϵ isoforms interact with phosphorylated tau.[18] Furthermore, different isoforms show distinct patterns of spatial, temporal, and subcellular distribution. The human θ and σ isoforms are predominantly expressed in T cells and epithelial cells, respectively.[14,19] The rat ϵ and γ isoforms are enriched in the synaptosomal membranes,[20] and the γ isoform is the main 14-3-3 protein located in the Golgi apparatus in mammalian cells.[3] In the developing rat brain, defined populations of neurons express β, γ, ζ, and θ isoforms at specific stages of development.[6,7] In the adult mouse brain, β, γ, η, and ζ isoforms are widely distributed with the localization primarily in neurons, although some glial cells express ϵ, θ, and ζ isoforms.[21]

Recently, several lines of evidence have indicated that the 14-3-3 protein is involved in neurodegenerative processes. The 14-3-3 protein detected in the cerebrospinal fluid of Creutzfeldt-Jacob disease has been used as a biochemical marker for the premortem diagnosis of Creutzfeldt-Jacob disease in the context of differential diagnosis of progressive dementia.[22–24] In addition, intense immunoreactivity against the ζ isoform was identified in amyloid plaques in the Creutzfeldt-Jacob disease brain.[25] However, several studies including our own showed that the 14-3-3 protein is occasionally detectable in the cerebrospinal fluid of infectious meningoencephalitis, metabolic encephalopathy, cerebrovascular diseases, and multiple sclerosis (MS) presenting with severe myelitis, suggesting that it is not a marker specific for prion diseases but for extensive destruction of brain tissues causing the leakage of 14-3-3 protein into the cerebrospinal fluid.[4,22,26,27] In the Alzheimer's disease brain, neurofibrillary tangles express immunoreactivity against the 14-3-3 protein.[28] The 14-3-3ζ homodimer interacts with tau and glycogen synthase kinase-3β (GSK3β), and stimulates GSK3β-mediated tau phosphorylation.[29] In the Parkinson's disease brain, Lewy bodies possess γ, ϵ, ζ, and θ isoforms that interact with α-synuclein.[30,31] Dopamine-dependent neurotoxicity is mediated by a soluble complex composed of the 14-3-3 protein and α-synuclein, whose levels are markedly elevated in the substantia nigra of the Parkinson's disease brain.[32] The neurotoxicity of ataxin-1, the causative protein of spinocerebellar ataxia type 1, is enhanced by ϵ and ζ isoforms that bind to and stabilize ataxin-1 phosphorylated by Akt, thereby slowing its degradation.[33] Finally, expression of the θ isoform is enhanced in the spinal cord of amyotrophic lateral sclerosis.[34] However, it remains unknown whether the 14-3-3 protein plays an active role in the pathological process of MS.

In the present study, we investigated the differential expression of seven 14-3-3 isoforms in chronic active demyelinating lesions of MS. We found that reactive astrocytes intensely express β, ϵ, ζ, η, and σ isoforms, among which the ϵ isoform provides a specific marker to identify reactive astrocytes in the MS brain. Furthermore, the 14-3-3 protein interacts with vimentin and glial fibrillary acidic protein (GFAP) in cultured human astrocytes. These observations suggest that the 14-3-3 protein plays an organizing role in the intermediate filament (IF) network in reactive astrocytes at the site of demyelinating lesions in MS.

Materials and Methods

MS and Non-MS Brain Tissues

Ten-μ-thick tissue sections were prepared from the brain, spinal cord, and optic nerve derived from four autopsy cases of MS numbered 791, 744, 609, and 544. The clinical and neuroradiological profiles of these patients are shown in a supplementary table on The American

Table 1. The14-3-3 Isoform-Specific or Broadly Reactive Antibodies Utilized for Immunochemistry and Western Blot Analysis

14-3-3 isoforms	Suppliers	Code	Antigen peptide	Origin	Specificity	Concentration used for immunohistiochemistry (μg/ml)	Concentration used for Western blotting (μg/ml)
Pan	SC	sc-629	N-terminal	Rabbit	Reactive to all isoforms	0.4	0.04
Pan	SC	sc-1657	N-terminal	Mouse	Reactive to all isoforms	0.4	0.04
β	SC	sc-628	C-terminal	Rabbit	Reactive predominantly to β isoform, but crossreactive to other isoforms to a lesser extent	0.4	0.04
β	IBL	18641	N-terminal	Rabbit	Not crossreactive to other isoforms	2	1
γ	IBL	18647	C-terminal	Rabbit	Not crossreactive to other isoforms	5	0.2
ϵ	IBL	18643	C-terminal	Rabbit	Not crossreactive to other isoforms	2	1
ζ	IBL	18644	N-terminal	Rabbit	Not crossreactive to other isoforms	2	0.5
η	IBL	18645	N-terminal	Rabbit	Not crossreactive to other isoforms	5	1
θ (τ)	SC	sc-732	C-terminal	Rabbit	Not crossreactive to other isoforms	0.4	0.04
θ (τ)	IBL	10017	Recombinant, whole	Mouse	Minimally crossreactive to σ isoform	1	1
σ	IBL	18642	C-terminal	Rabbit	Not crossreactive to other isoforms	1	1

Abbreviations: SC, Santa Cruz Biotechnology; IBL, Immunobiological Laboratory. The specificity of the antibodies (IBL) is also shown on Supplementary Figure 1 at *http://www.amjpathol.org*.

Journal of Pathology website (*http://www.amjpathol.org*). The tissues were fixed with 4% paraformaldehyde (PFA) or 10% neutral formalin and embedded in paraffin. For the controls, tissue sections were prepared from the autopsied brains of six non-MS neurological and psychiatric disease cases that include a 47-year-old man with acute cerebral infarction who died of sepsis (no. 719), an 84-year-old man with acute cerebral infarction who died of disseminated intravascular coagulation (no. 786), a 62-year-old man with old cerebral infarction who died of pancreatic cancer (no. 789), a 56-year-old man with old cerebral infarction who died of myocardial infarction (no. 807), a 36-year-old woman with schizophrenia who died of lung tuberculosis (no. 523), and a 61-year-old man with schizophrenia who died of asphyxia (no. 826). In addition, they were prepared from the autopsied brains of six neurologically normal patients that include a 79-year-old woman who died of hepatic cancer (no. G6), a 75-year-old woman who died of breast cancer (no. G7), a 60-year-old woman who died of external auditory canal cancer (no. G8), a 74-year-old woman who died of gastric and hepatic cancers (no. G9), an 83-year-old woman who died of gastric cancer and myocardial infarction (no. A2623), and a 65-year-old man who died of liver cirrhosis and bronchopneumonia (no. A2647). Autopsies on all patients were performed at the National Center Hospital for Mental, Nervous, and Muscular Disorders, NCNP, Tokyo, Japan. Written informed consent was obtained in all cases.

Immunohistochemistry and Immunocytochemistry

After deparaffination, the tissue sections were heated by microwave at 95°C for 10 minutes in 10 mmol/L citrate sodium buffer (pH 6.0). They were then treated at room temperature for 15 minutes with 3% H_2O_2-containing methanol. For vimentin immunolabeling, the tissue sections were pretreated with 0.125% trypsin solution (Nichirei, Tokyo, Japan) at 37°C for 15 minutes. They were then incubated with 10% normal goat serum containing phosphate-buffered saline (PBS) at room temperature for 15 minutes to block nonspecific staining. The sections were incubated in a moist chamber at 4°C overnight with a panel of 14-3-3 isoform-specific antibodies or with antibodies broadly reactive against all isoforms listed in Table 1. The antibodies were obtained from Immunobiological Laboratory (IBL), Gumma, Japan, and Santa Cruz Biotechnology, Santa Cruz, CA. The specificity of the antibodies from IBL is shown in Supplementary Figure 1 on The American Journal of Pathology website, and additional information on those of Santa Cruz Biotechnology is available on the supplier's website (*www.scbt.com*). After washing with PBS, the tissue sections were labeled at room temperature for 30 minutes with peroxidase-conjugated secondary antibodies (Simple Stain MAX-PO kit, Nichirei) followed by incubation with a colorizing solution containing diaminobenzidine tetrahydrochloride and a counterstain with hematoxylin. To identify cell types expressing the 14-3-3 protein, adjacent sections were stained with the following antibodies: rabbit polyclonal antibody against GFAP (N1506; DAKO, Carpinteria, CA), rabbit polyclonal antibody against vimentin (H-84; Santa Cruz Biotechnology), mouse monoclonal antibody against vimentin (V9; Santa Cruz Biotechnology), rabbit polyclonal antibody against myelin basic protein (N1546; DAKO), mouse monoclonal antibody against CD68 (N1577; DAKO), and mouse monoclonal antibody against 70-kd and 200-kd neurofilament proteins (2F11; Nichirei). For negative controls, sections were incubated with a rabbit-negative control reagent (DAKO) instead of primary antibodies. The optimum concentrations of these antibodies and incubation periods were determined according to the supplier's instruction.

For double-labeling immunocytochemistry, cells on cover glasses were fixed with 4% PFA in 0.1 mol/L phos-

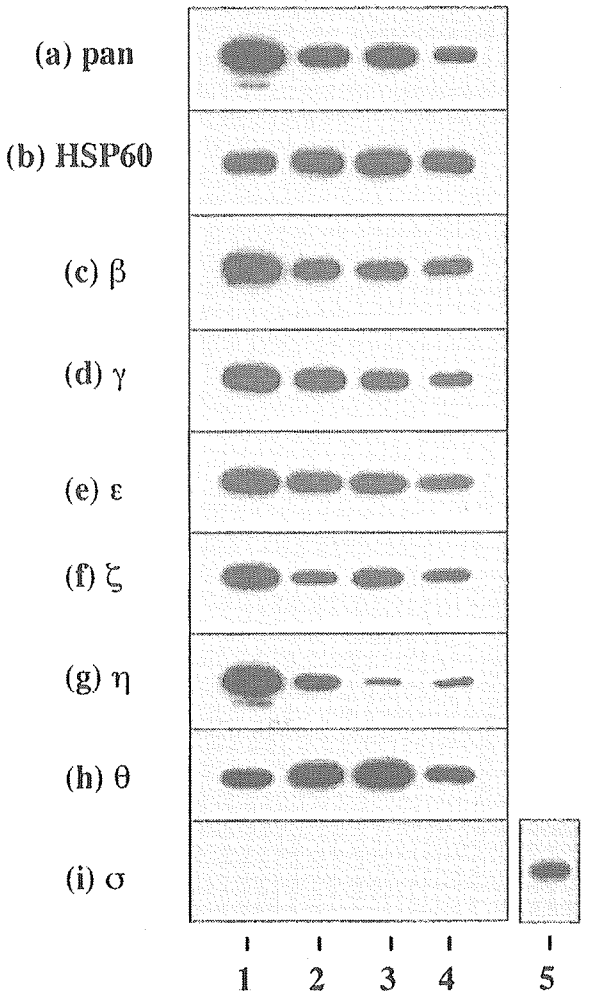

Figure 1. Constitutive expression of 14-3-3 isoforms in cultured human cells. Two μg of total protein extract isolated from brain tissues or cultured cells incubated in 10% FBS-containing medium were processed for Western blot analysis using a battery of 14-3-3 isoform-specific antibodies or the antibodies broadly reactive against all of the isoforms listed in Table 1, or the antibody against the housekeeping gene product HSP60. **a** to **i** indicate the following antibody specificity: **a**, all isoforms; **b**, HSP60; **c**, β; **d**, γ; **e**, ε; **f**, ζ; **g**, η; **h**, θ; and **i**, σ. **Lanes 1** to **4** represent homogenate of the human cerebrum (**lane 1**), NTera2-derived differentiated neurons (NTera2-N) (**lane 2**), U-373MG astrocytoma cells (**lane 3**), fetal human astrocytes (AS1477) (**lane 4**), and HeLa cervical carcinoma cells (**lane 5**).

phate buffer (pH 7.4) at room temperature for 10 minutes, followed by incubation with PBS containing 0.5% Triton X-100 at room temperature for 20 minutes.[26] The cells were then incubated at room temperature for 30 minutes with a mixture of 14-3-3 isoform-specific antibody and rat monoclonal anti-GFAP antibody (2.2B10) or V9 antibody. Next, they were incubated at room temperature for 30 minutes with a mixture of rhodamine-conjugated anti-rabbit IgG and fluorescein isothiocyanate-conjugated anti-rat or mouse IgG (ICN-Cappel, Aurora, OH). After several washes, cover glasses were mounted on the slides with glycerol-polyvinyl alcohol, and the slides were examined under a Nikon ECLIPSE E800 universal microscope equipped with fluorescein and rhodamine optics. Negative controls were processed following these steps except for exposure to primary antibody.

Cell Culture

Two different sources of cultured human astrocytes were used. One was fetal human astrocytes named AS1477, provided by Drs. K. Watabe and S. U. Kim of the University of British Columbia, Vancouver, BC, Canada. They were maintained in Dulbecco's modified Eagle's medium (DMEM) supplemented with 10% fetal bovine serum (FBS), 100 U/ml penicillin, and 100 μg/ml streptomycin (feeding medium). The other was astrocytes named AS-BW, whose differentiation was induced from neuronal progenitor (NP) cells. NP cells isolated from the brain of a human fetus at 18.5 weeks of gestation were obtained from BioWhittaker (Walkersville, MD). NP cells plated on a polyethyleneimine-coated surface were incubated in DMEM/F-12 medium containing an insulin-transferrin-selenium supplement (Invitrogen, Carlsbad, CA), 20 ng/ml recombinant human epidermal growth factor (Higeta, Tokyo, Japan), 20 ng/ml recombinant human basic fibroblast growth factor (PeproTech EC, London, UK), and 10 ng/ml recombinant human leukemia inhibitory factor (Chemicon, Temecula, CA) (NP medium).[35] For the induction of astrocyte differentiation, NP cells were incubated for several weeks in feeding medium instead of NP medium. This incubation induced vigorous proliferation and differentiation of astrocytes accompanied by a rapid reduction in nonastroglial cell types. Newborn mouse astrocytes were prepared as previously described.[26] In some experiments, cultured human and mouse astrocytes were plated at subconfluent density and incubated for 7 days in serum-free DMEM/F-12 medium supplemented with insulin-transferrin-selenium without inclusion of any other growth factors or in 10% FBS-containing DMEM/F-12 medium supplemented with insulin-transferrin-selenium.

Human cell lines such as U-373MG astrocytoma, NTera2 teratocarcinoma and HeLa cervical carcinoma were obtained from the RIKEN Cell Bank (Tsukuba, Japan) and the American Type Culture Collection (Rockville, MD). For the induction of neuronal differentiation, NTera2 cells maintained in the undifferentiated state (NTera2-U) were incubated for 4 weeks in feeding me-

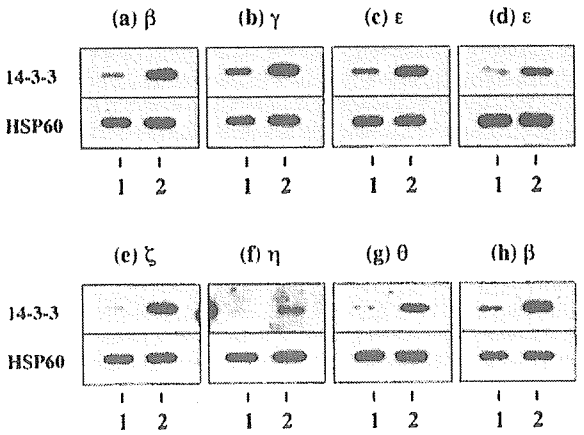

Figure 2. Growth-dependent expression of various 14-3-3 isoforms in cultured human astrocytes. Human and mouse astrocytes were plated at subconfluent density and incubated for 7 days in the serum-free culture medium or in 10% FBS-containing culture medium. Two μg of total protein extract was processed for Western blot analysis using a battery of 14-3-3 isoform-specific antibodies or with the antibodies broadly reactive against all isoforms (**top**). After stripping the antibodies, identical blots were relabeled with the antibody against HSP60 for the standardization of expression levels (**bottom**). **a** to **g** (**top**) indicate the expression of β (**a**), γ (**b**), ε (**c**), ζ (**e**), η (**f**), and θ (**g**) in human astrocytes (AS1477); ε in human astrocytes (AS-BW) (**d**); and β in mouse astrocytes (**h**). **Lanes 1** and **2** represent the cells cultured under the serum-free growth-arrested condition (**lane 1**) or the serum-containing growth-promoting condition (**lane 2**). Additional data are shown in supplementary Figure 2 on the American Journal of Pathology website.

Table 2. Differential Expression of Seven 14-3-3 Isoforms in Glial Cells and Neurons in MS and Control Brains

Brains 14-3-3 isoforms/cell types	Astrocytes			Microglia/macrophages			Oligodendrocytes			Neurons		
	MS	OND	NNC	MS	OND	NNC	MS	OND	NNC	MS	OND	NNC
β	maj (++)	maj (+)	no (−)	maj (++)	maj (++)	no (−)	min (+)	no (−)	no (−)	maj (++)	maj (++)	maj (++)
γ	min (++)	min (+)	no (−)	min (++)	min (+)	no (−)	no (−)	no (−)	no (−)	maj (++)	maj (++)	maj (++)
ε	maj (++)	maj (++)	min (+)	no (−)	no (−)	no (−)	no (−)	no (−)	no (−)	min (+)	min (+)	min (+)
ζ	maj (++)	maj (++)	no (−)	maj (++)	maj (++)	no (−)	no (−)	no (−)	no (−)	maj (++)	maj (++)	maj (++)
η	maj (++)	maj (++)	no (−)	maj (++)	min (++)	no (−)	no (−)	no (−)	no (−)	maj (++)	maj (++)	maj (++)
θ	min (+)	min (+)	no (−)	no (−)	no (−)	no (−)	min (++)	min (++)	min (+)	min (+)	min (+)	min (+)
σ	min (++)	min (++)	min (+)	no (−)	no (−)	no (−)	no (−)	no (−)	no (−)	no (−)	no (−)	no (−)

The present study includes four MS cases numbered #791, 744, 609, and 544 whose clinical profiles are given in a supplementary table on the AJP website, six non-MS neurological and psychiatric disease cases (OND) composed of #719 acute cerebral infarction, #786 acute cerebral infarction, #789 old cerebral infarction, #807 old cerebral infarction, #523 schizophrenia, and #826 schizophrenia, and six neurologically normal cases (NNC) composed of #G6, #G7, #G8, #G9, #A2623, and #A2647, whose profiles are described in the Materials and Methods section.

The population size of the immunoreactive cells is expressed as maj, major (large) population; min, minor (small) population; and no, almost no population. The intensity of immunoreactivity is graded as (−) negative, (+) weak, and (++) intense.

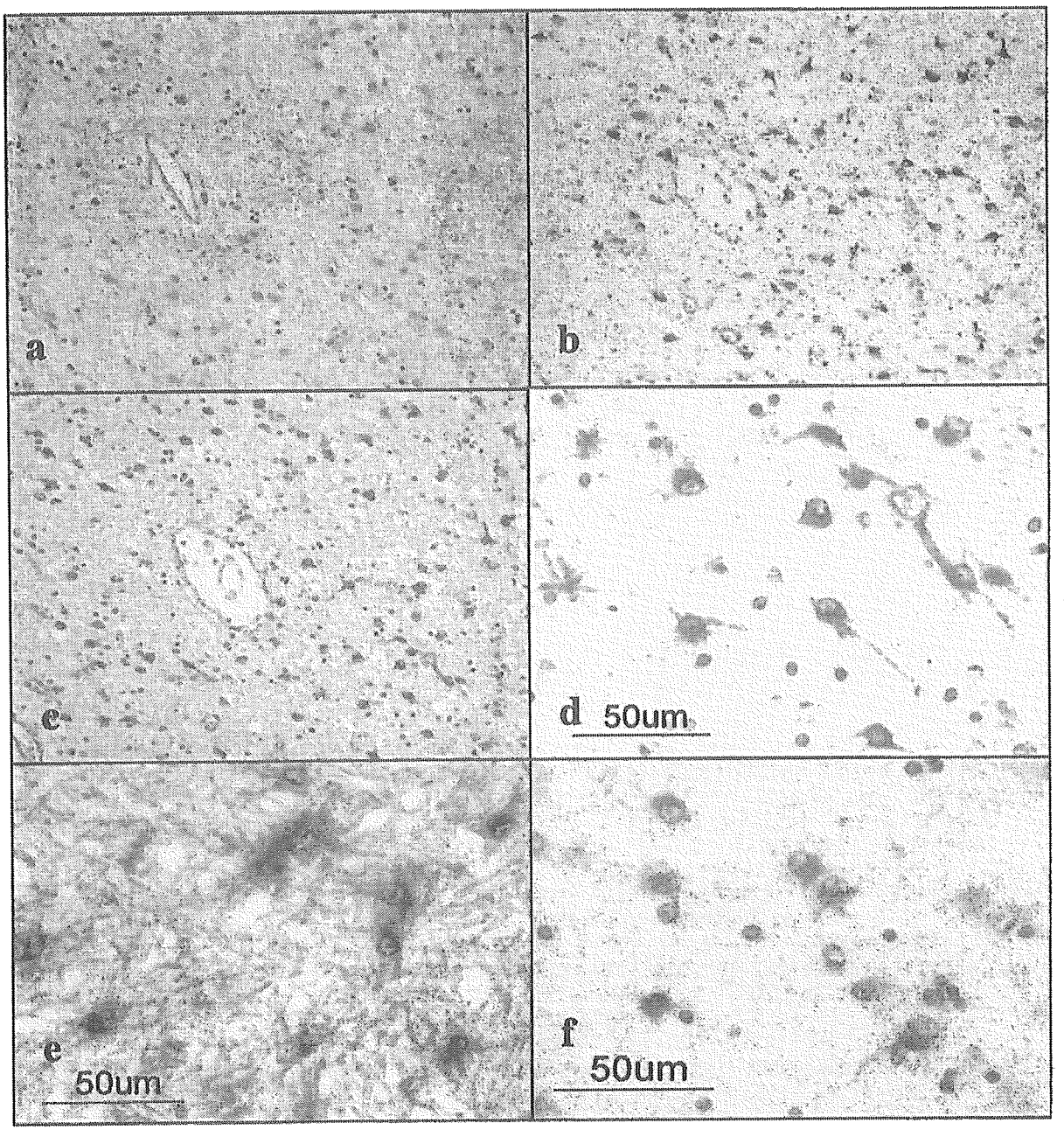

Figure 3. The 14-3-3 ε isoform is expressed in reactive astrocytes in chronic demyelinating lesions of MS. MS brain tissues were processed for immunohistochemical analysis using ε isoform-specific antibody or the antibody against GFAP or vimentin. **a** to **f** represent the following: **a:** no. 744 MS, chronic active demyelinating lesions in the subcortical white matter of the frontal lobe (H&E). **b:** No. 744 MS, the area corresponding to **a** (GFAP). Many reactive astrocytes are stained. **c:** No. 744 MS, the area corresponding to **a** (ε). Many reactive astrocytes are stained. **d:** No. 744 MS, a higher magnification view of **c** (ε). Reactive astrocytes are stained. **e:** No. 544 MS, chronic inactive demyelinating lesions in the optic nerve (ε). Reactive astrocytes and the glial scar are stained. **f:** No. 744 MS, chronic active demyelinating lesions in the subcortical white matter of the frontal lobe (vimentin). Reactive astrocytes are stained.

dium containing 10^{-5} mol/L *all trans* retinoic acid (Sigma, St. Louis, MO), replated twice and then plated on a surface coated with Matrigel Basement Membrane Matrix (Becton Dickinson, Bedford, MA). They were incubated for another 2 weeks in feeding medium containing a cocktail of mitotic inhibitors, resulting in the enrichment of differentiated neurons (NTera2-N).[36]

Western Blot Analysis

To prepare total protein extract for Western blot analysis, the cells and tissues were homogenized in RIPA lysis buffer composed of 50 mmol/L Tris-HCl (pH 7.5), 150 mmol/L NaCl, 1% Nonidet P-40, 0.5% sodium deoxycholate, 0.1% sodium dodecyl sulfate (SDS), and a cock-

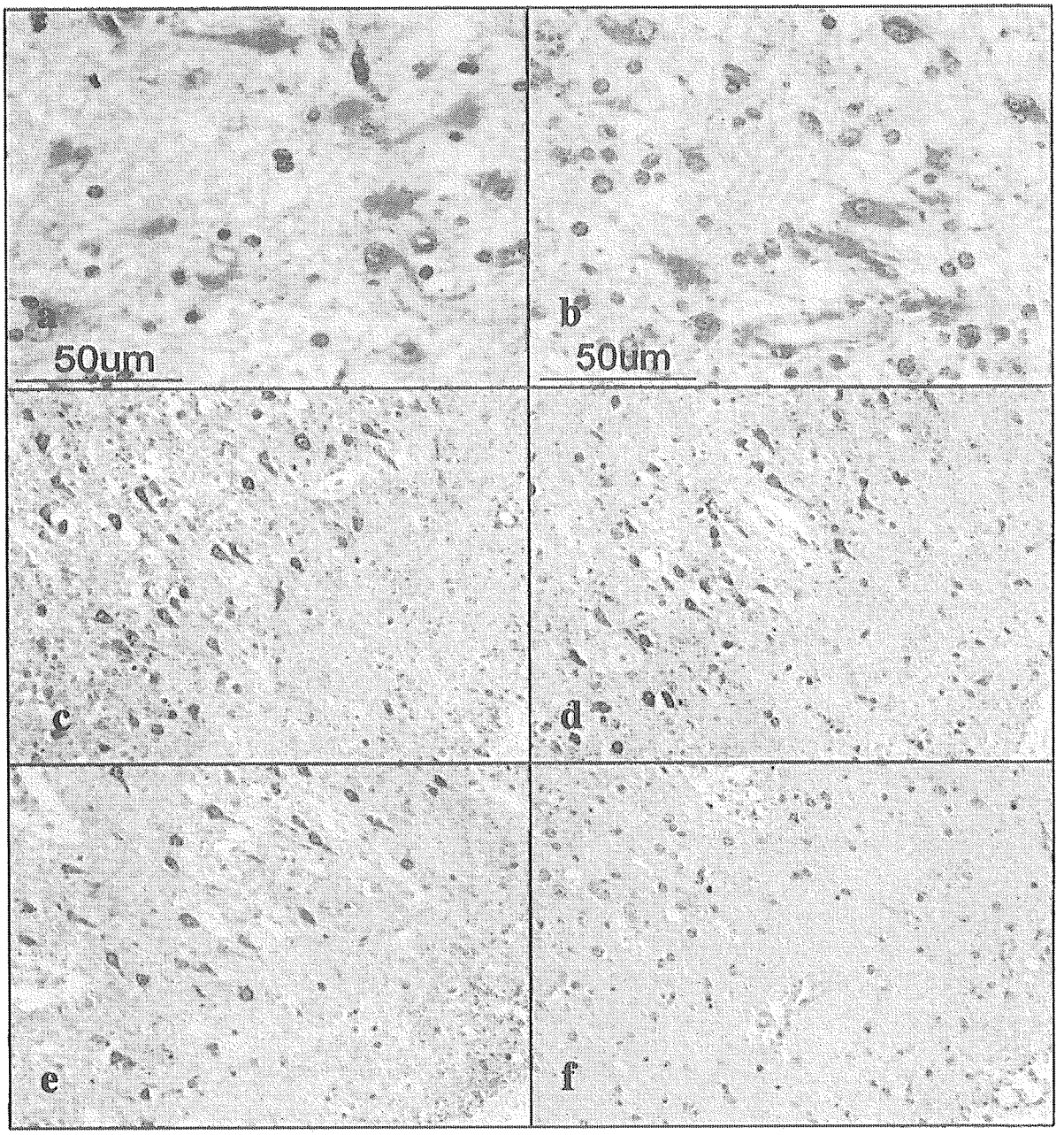

Figure 4. Expression of various 14-3-3 isoforms in reactive astrocytes and cortical neurons in MS brain. MS brain tissues were processed for immunohistochemical analysis using a battery of 14-3-3 isoform-specific antibodies. **a** to **f** represent the following: **a:** no. 744 MS, chronic active demyelinating lesions in the subcortical white matter of the frontal lobe (β). Reactive astrocytes are stained. **b:** No. 744 MS, chronic active demyelinating lesions in the subcortical white matter of the frontal lobe (ζ). Reactive astrocytes are stained. **c:** No. 744 MS, the cerebral cortex of the frontal lobe (γ). Cortical neurons are stained. **d:** No. 744 MS, the area corresponding to **c** (η). Cortical neurons are stained. **e:** No. 744 MS, the area corresponding to **c** (ζ). Cortical neurons are stained. **f:** No. 744 MS, the area corresponding to **c** (ϵ). Cortical neurons are devoid of staining.

tail of protease inhibitors (Roche Diagnositics, Mannheim, Germany), followed by centrifugation at 12,000 rpm at room temperature for 20 minutes. The supernatant was collected for separation on a 12% SDS-polyacrylamide gel electrophoresis (PAGE) gel and the protein concentration was determined by a Bradford assay kit (Bio-Rad, Hercules, CA). After gel electrophoresis, the protein was transferred onto nitrocellulose membranes and immunolabeled at room temperature overnight with a panel of anti-14-3-3 protein antibodies listed in Table 1. Then, the membranes were incubated at room temperature for 30 minutes with horseradish peroxidase-conjugated anti-rabbit IgG or anti-mouse IgG (Santa Cruz Biotechnology). The specific reaction was visualized with a Western blot detection system using a chemiluminescent substrate (Pierce, Rockford, IL). After the antibodies were stripped

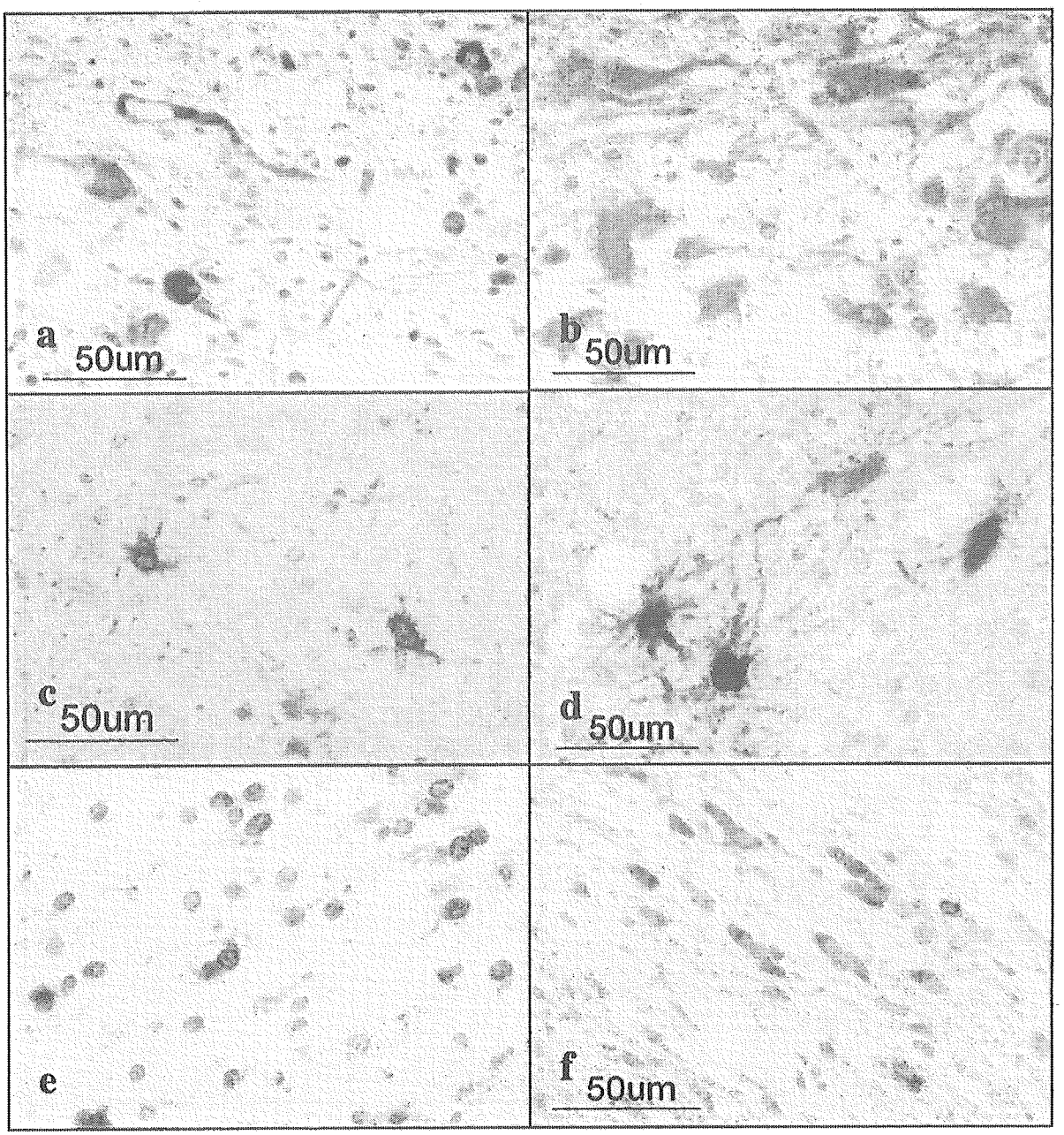

Figure 5. Expression of various 14-3-3 isoforms in reactive astrocytes, surviving oligodendrocytes, and injured axons in chronic demyelinating lesions of MS and in infarcted lesions. The brains of MS and non-MS control cases were processed for immunohistochemical analysis using a battery of 14-3-3 isoform-specific antibodies. **a** to **f** represent the following: **a:** no. 609 MS, chronic active demyelinating lesions in the medulla oblongata (γ). Disrupted axons are stained. **b:** No. 719 acute cerebral infarction, infarcted lesions in the parietal cerebral cortex (ϵ). Reactive astrocytes are stained. **c:** No. 791 MS, chronic inactive lesions in the pons (σ). Reactive astrocytes are stained. **d:** No. 719 acute cerebral infarction, infarcted lesions in the parietal cerebral cortex (σ). Reactive astrocytes are stained. **e:** No. 609 MS, chronic active demyelinating lesions in the periventricular white matter of the frontal lobe (θ). Surviving oligodendrocytes are stained. **f:** No. 744 MS, chronic active demyelinating lesions in the optic nerve (θ). Surviving oligodendrocytes are stained.

by incubating the membranes at 50°C for 30 minutes in stripping buffer composed of 62.5 mmol/L Tris-HCl (pH 6.7), 2% SDS, and 100 mmol/L 2-mercaptoethanol, the membranes were processed for relabeling with goat polyclonal antibody against human heat shock protein HSP60 (N-20; Santa Cruz Biotechnology) followed by incubation with horseradish peroxidase-conjugated anti-goat IgG (Santa Cruz Biotechnology). Densitometric analysis was performed using NIH image version 1.61 software to quantify the intensity of the immunoreactive bands.[36]

Immunoprecipitation Experiments

To prepare total protein extract for immunoprecipitation experiments, the cells were homogenized in M-PER lysis buffer (Pierce) with a cocktail of protease inhibitors fol-

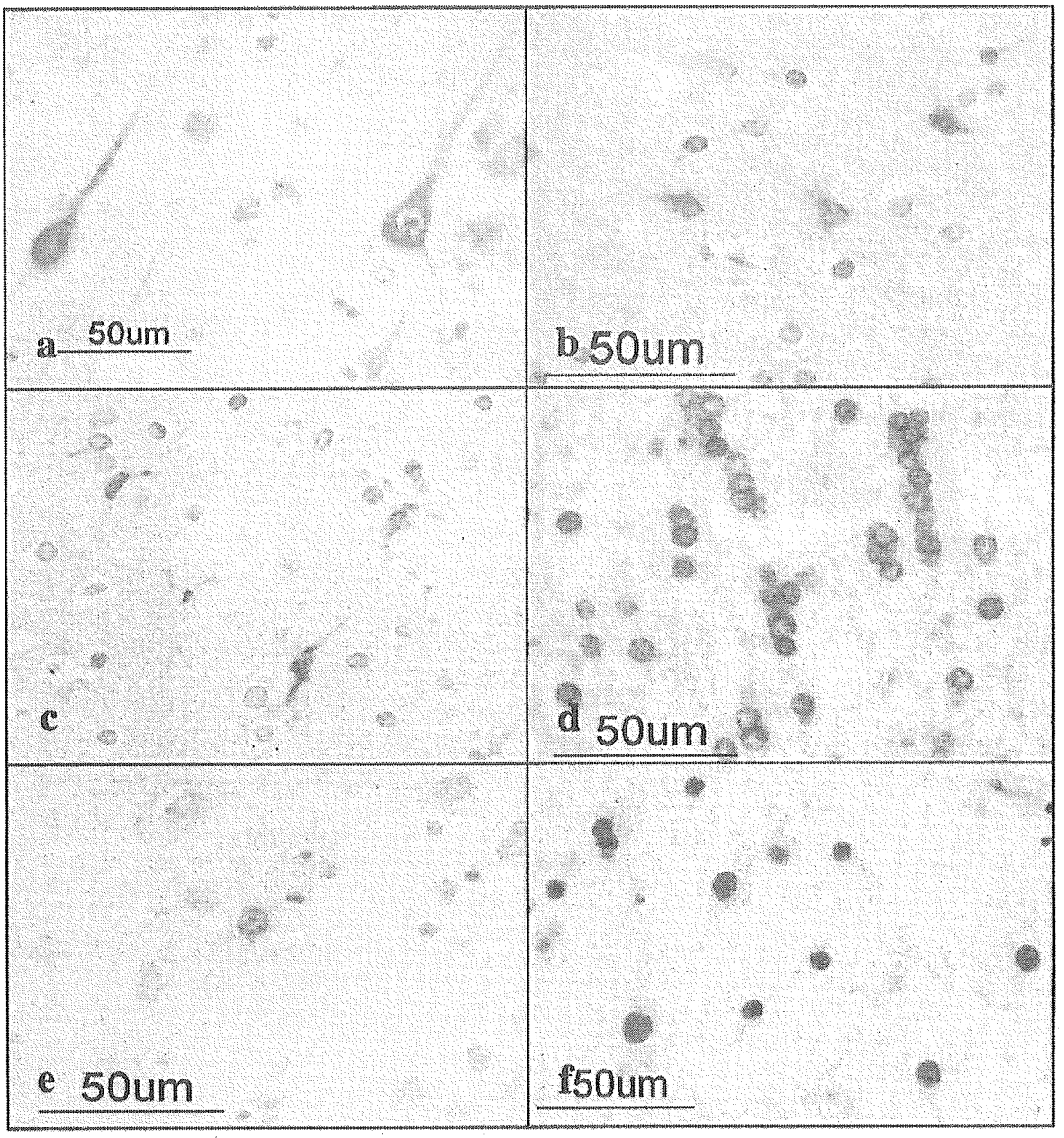

Figure 6. Expression of various 14-3-3 isoforms in neurons, astrocytes, oligodendrocytes, and microglia in non-MS brains. The brains of non-MS control cases were processed for immunohistochemical analysis using a battery of 14-3-3 isoform-specific antibodies. **a** to **f** represent the following: **a:** no. G9 neurologically normal subject, the frontal cerebral cortex (γ). Cortical neurons are stained. **b:** No. 523 schizophrenia, frontal cerebral cortex (ϵ). Astrocytes are stained. **c:** No. 826 schizophrenia, the frontal cerebral cortex (η). Microglia are stained. **d:** No. 786 acute cerebral infarction, the subcortical white matter of the parietal lobe (θ). Surviving oligodendrocytes are stained. **e:** No. G7 neurologically normal subject, the frontal cerebral cortex (σ). A few astrocytes are stained. **f:** No. 789 old cerebral infarction, the frontal cerebral cortex (ϕ). The nuclei of reactive astrocytes are stained.

lowed by centrifugation at 12,000 rpm at room temperature for 20 minutes. After preclearance, the supernatant was incubated at 4°C for 1 hour with a panel of anti-14-3-3 protein antibodies or the same amount of normal rabbit IgG (Santa Cruz Biotechnology). It was then incubated with Protein G Sepharose (Amersham Bioscience, Piscataway, NJ). After several washes, the immunoprecipitates were processed for Western blot analysis using V9 antibody or mouse monoclonal antibody against GFAP (GA5; Nichrei).

Two-Dimensional Gel Electrophoresis and Mass Spectrometry Analysis

To prepare total protein extract for two-dimensional gel electrophoretic analysis, the cells were homogenized in

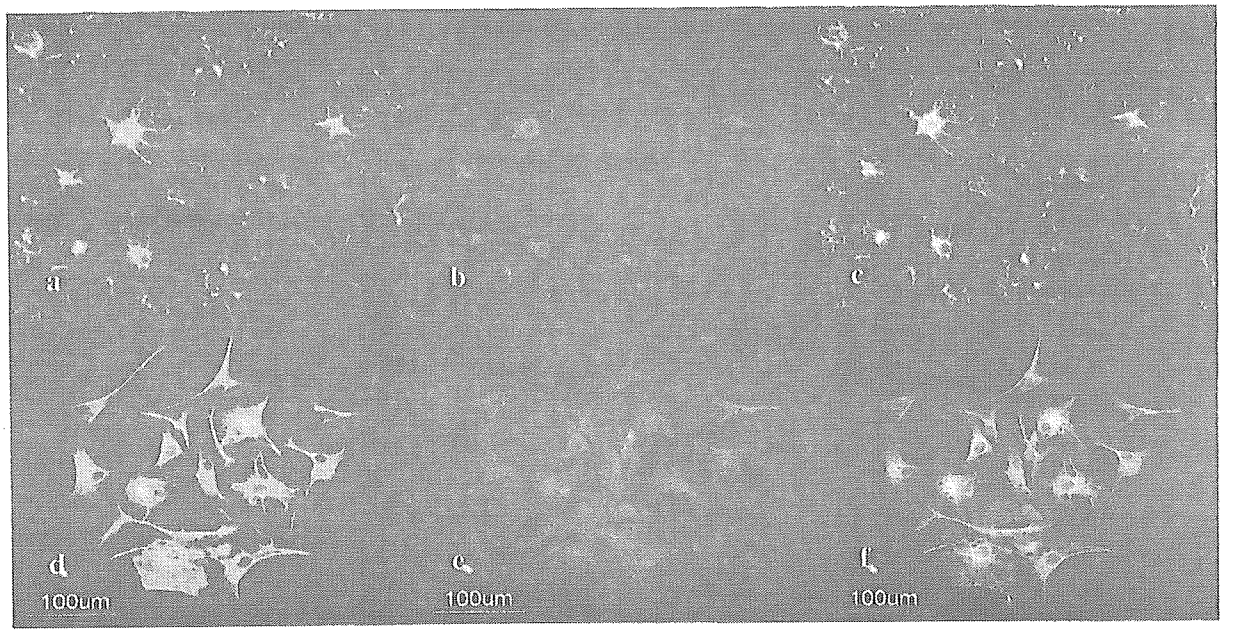

Figure 7. Co-expression of the 14-3-3 ε isoform and GFAP in reactive astrocytes in chronic demyelinating lesions of MS and in cultured human astrocytes. Cultured human astrocytes and MS brain tissues were processed for double immunolabeling with anti-GFAP antibody and ε isoform-specific antibody followed by labeling with fluorescein isothiocyanate- and rhodamine-conjugated secondary antibodies. **a** to **f** represent no. 744, chronic active demyelinating lesions in the subcortical white matter of the frontal lobe (**a–c**), cultured human astrocytes (AS-BW) (**d–f**), GFAP (**a**, **d**), ε (**b**, **e**), and the overlay (**c**, **f**).

rehydration buffer composed of 8 mol/L urea, 2% CHAPS, 0.5% carrier ampholytes (pH 4 to 6), 20 mmol/L dithiothreitol, 0.002% bromophenol blue, and a cocktail of protease inhibitors and phosphatase inhibitors (Sigma). Urea-soluble protein was separated by isoelectric focusing using the ZOOM IPGRunner system (Invitrogen) loaded with an immobilized pH 4.5 to 5.5 gradient strip. After the first dimension of isoelectric focusing, the protein was separated in the second dimension on a NuPAGE 4 to 12% polyacrylamide gel (Invitrogen). The gel was stained using Coomassie brilliant blue G-250 solution or the Silverquest silver staining kit (Invitrogen). It was transferred onto a polyvinylidene difluoride membrane for protein overlay and Western blot analysis. Spots of interest were excised from the gels, trypsinized, and processed for mass spectrometry (nanoESI-MS/MS) analysis followed by database searching using MASCOT software (Invitrogen Proteome, Yokohama, Japan).

Protein Overlay Analysis

To prepare the 14-3-3 protein-specific probe for protein overlay analysis, the open reading frame of the human 14-3-3ε isoform gene (YWHAE, GenBank accession No. NM_006761) was amplified from the cDNA of NTera2-N cells by the polymerase chain reaction using sense and anti-sense primers (5′atggatgatcgagaggatctggtg3′ and 5′tcactgattttcgtcttccacgtc3′). The polymerase chain reaction product was cloned into a prokaryotic expression vector pTrcHis-TOPO (Invitrogen). The expression of recombinant human 14-3-3ε protein having an N-terminal Xpress tag for detection (rh14-3-3ε) was induced in *Escherichia coli* by exposure to isopropyl β-thiogalactoside. The recombinant protein was further purified through a HiTrap chelating HP column (Amersham Bioscience) and by separation on a 12% SDS-PAGE gel. Recombinant human interferon-stimulated protein ISG15 fused to an N-terminal Xpress tag (rhISG15), a vimentin-binding protein in human cancer cells,[37] was prepared for the control probe. The polyvinylidene difluoride membrane on which the gel was blotted was incubated at room temperature overnight with 1 μg/ml rh14-3-3ε or rhISG15 probe, followed by immunolabeling with mouse monoclonal anti-Xpress antibody (Invitrogen) and horseradish peroxidase-conjugated anti-mouse IgG. After the probes and antibodies were stripped by incubating the membrane at 50°C for 30 minutes in stripping buffer, it was repeatedly relabeled with V9 antibody, GA5 antibody, or rabbit polyclonal antibodies specific for phosphorylated Ser-39, Ser-72, or Ser-83 epitopes of vimentin (Santa Cruz Biotechnology), followed by incubation with horseradish peroxidase-conjugated anti-mouse or rabbit IgG.

Results

Growth-Dependent Expression of 14-3-3 Isoforms in Cultured Human Astrocytes

To investigate the expression pattern of seven 14-3-3 isoforms in human neural cells, cultured human astrocytes, NTera2-N neurons, and U-373MG astrocytoma cells, all of which were incubated in 10% FBS-containing culture medium, were processed for Western blot analysis using a panel of isoform-specific antibodies or the antibodies broadly reactive against all of the isoforms listed in Table 1. Cultured human astrocytes, neurons, and astrocytoma cells, along with

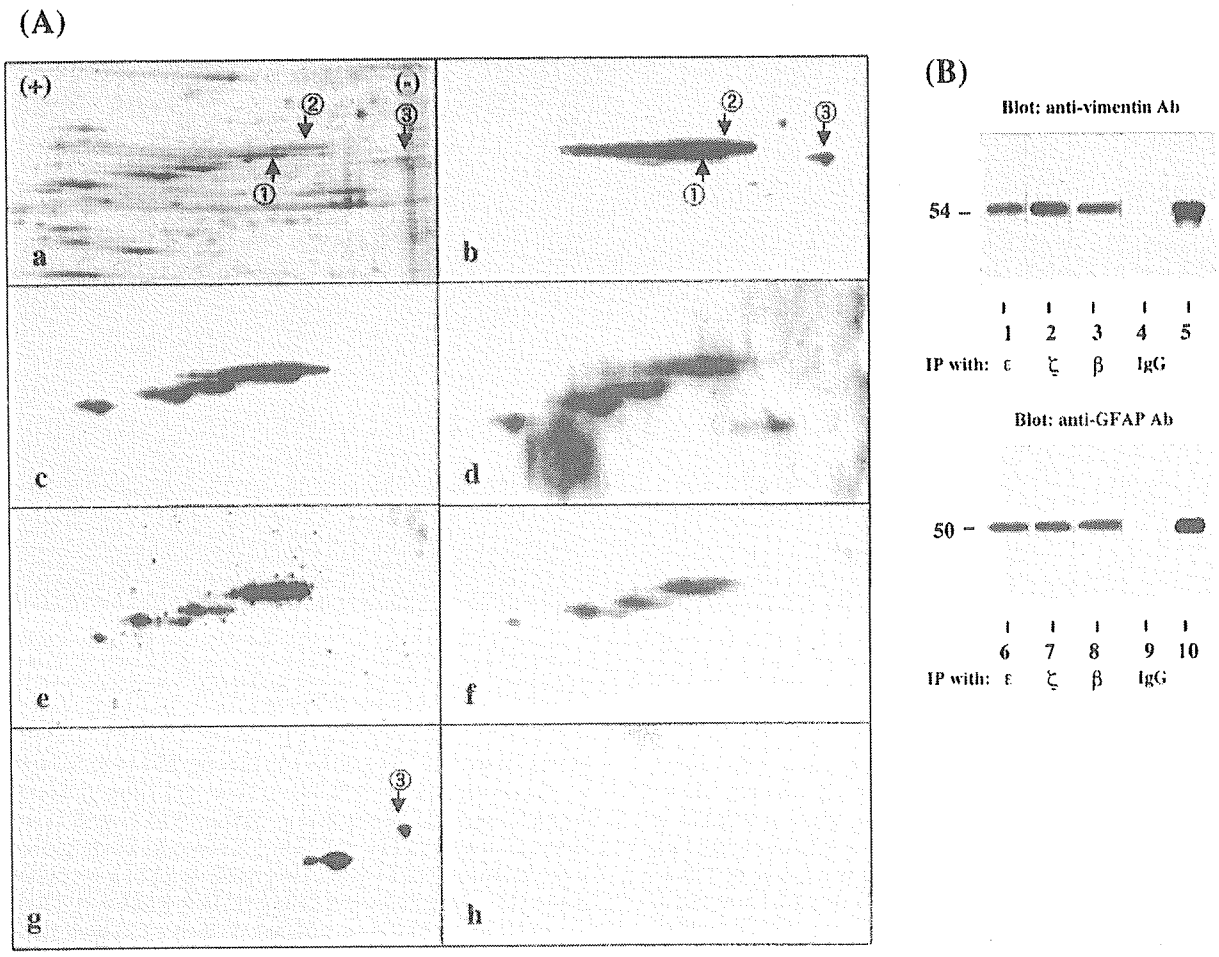

Figure 8. Two-dimensional gel electrophoresis and immunoprecipitation analysis of 14-3-3 ε isoform-binding proteins in cultured human astrocytes. **A:** Two-dimensional gel analysis. Human astrocytes (AS-BW) were incubated in 10% FBS-containing culture medium. Twenty-one μg of total protein extract was separated on a two-dimensional PAGE gel, transblotted onto a polyvinylidene difluoride membrane, and processed for overlay analysis with recombinant human 14-3-3ε protein possessing the Xpress tag (rh14-3-3ε) followed by labeling with anti-Xpress antibody. After the probe and antibody were stripped, the blot was repeatedly relabeled six times with the antibodies against GFAP, vimentin, and vimentin with specific phosphorylated serine epitopes, and with recombinant human interferon-stimulated protein ISG15 having the Xpress tag (rhISG15). **a** to **g** represent silver staining (**a**), rh14-3-3ε labeling followed by staining with anti-Xpress antibody (**b**), vimentin (**c**), vimentin with phosphorylated Ser-39 (**d**), vimentin with phosphorylated Ser-72 (**e**), vimentin with phosphorylated Ser-83 (**f**), GFAP (**g**), and rhISG15 labeling followed by staining with anti-Xpress antibody (**h**). Two major spots labeled with rh14-3-3ε and anti-vimentin antibody are named spot no. 1 and no. 2, while a spot labeled with rh14-3-3ε and anti-GFAP antibody is designated spot no. 3. Spots no. 1 and no. 2 were excised from the gel and processed for mass spectrometry (MS) analysis. **B:** Immunoprecipitation analysis. Total protein extract of cultured human astrocytes was immunoprecipitated with ε isoform-specific antibody (**lanes 1** and **6**), ζ isoform-specific antibody (**lanes 2** and **7**), β-isoform-specific antibody (**lanes 3** and **8**), with the same amount of normal rabbit IgG (**lanes 4** and **9**), or untreated with any antibodies (**lanes 5** and **10**; 2 μg of total protein extract before processing for immunoprecipitation). Then, the immunoprecipitates were processed for Western blot analysis using anti-vimentin (**top**) or anti-GFAP antibody (**bottom**).

human brain homogenate, expressed substantial levels of β, γ, ε, ζ, η, and θ isoforms (Figure 1, a to h; lanes 1 to 4). In contrast, the σ isoform was undetectable in human neural cells but was identified in HeLa cells (Figure 1i, lanes 1 to 5).

To study the effects of culture conditions on 14-3-3 protein levels, human astrocytes were incubated for 7 days in 10% FBS-containing culture medium or in the serum-free culture medium, which led to nearly complete growth arrest. The expression levels of β, γ, ε, ζ, η, and θ isoforms were elevated in human astrocytes incubated in the serum-containing growth-promoting condition. The expression was enhanced 3.3-, 1.6-, 2.2-, 10.0-, 18.7-, or 4.6-fold, respectively, compared with the levels under the serum-free growth-arrested condition when standardized against the levels of HSP60, a housekeeping gene product on the identical blots (Figure 2, a to c, e to g; top and bottom panels, lanes 1 and 2). The serum-induced up-regulation of 14-3-3 isoforms was also observed in a different culture of human astrocytes (Figure 2d, top and bottom panels, lanes 1 and 2) and mouse astrocytes in culture (Figure 2h, top and bottom panels, lanes 1 and 2; and additional data shown in Supplementary Figure 2 on The American Journal of Pathology website at *http://www.amjpathol.org*). These results indicate that cultured human astrocytes constitutively express all iso-

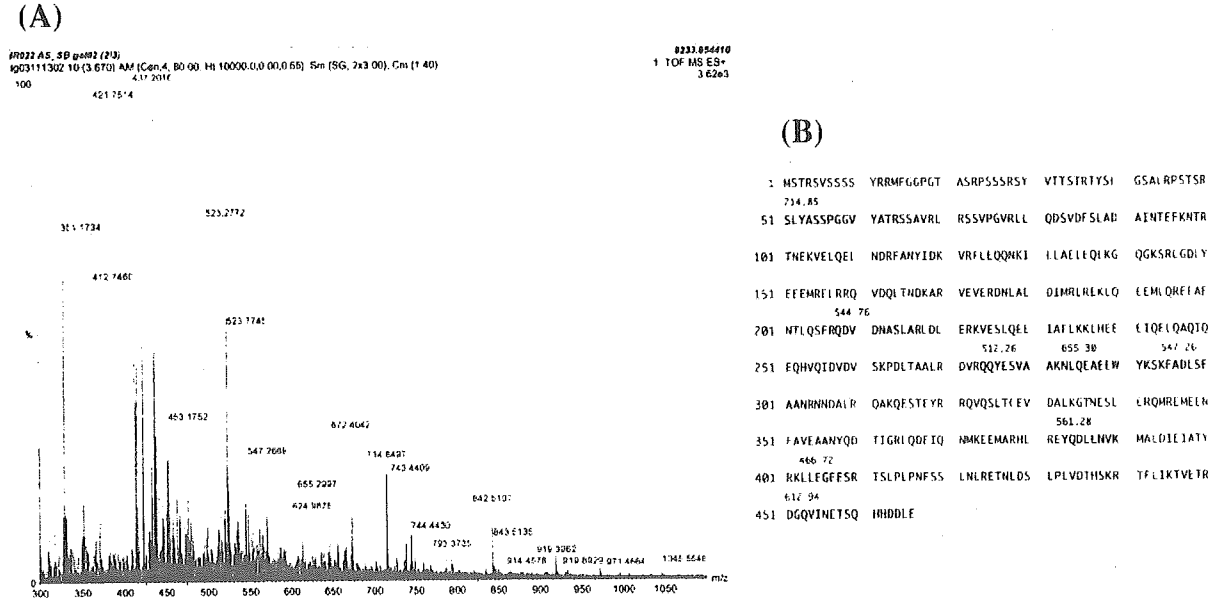

Figure 9. Mass spectrometry analysis of the 14-3-3 ε isoform-binding proteins in cultured human astrocytes. Spots no. 1 and no. 2 labeled with the rh14-3-3ε probe (Figure 8A, a and b) were excised from the gel, trypsinized, and processed for nanoESI-MS/MS analysis. **A:** The spectra of nanoESI-MS/MS analysis of spot no. 1. Each peak indicates individual peptide fragments. The position of several peaks was automatically numbered on the spectra. Peptides derived from the autolytic fragments of trypsin (eg. 412, 421, and 523) were omitted to be processed for further analysis. The peptide fragments were selected for MS analysis in order of their signal intensity. **B:** Amino acid sequence of human vimentin. Eight peptide fragments of spot no. 1 identified by nanoESI-MS/MS analysis (**shadowed**) showed a perfect match with the amino acid sequence encompassing residues 51 to 466 of vimentin. The number indicated on each fragment represents the position in the horizontal axis of the spectra (**A**).

forms except for σ, whose levels were elevated in a cell growth-dependent manner.

Differential Expression of 14-3-3 Isoforms in Reactive Astrocytes in Demyelinating Lesions of MS

To investigate the differential expression of seven 14-3-3 isoforms in MS lesions, the brain, spinal cord, and optic nerve of four progressive MS patients (no. 791, no. 744, no. 609, and no. 544) and 12 non-MS control cases were processed for immunohistochemistry using a panel of isoform-specific antibodies. In chronic active and inactive demyelinating lesions of MS, the majority of GFAP$^+$ hypertrophic astrocytes intensely expressed β, ϵ, ζ, and η isoforms, whereas a small population of reactive astrocytes displayed immunoreactivities against γ, θ, and σ isoforms (Table 2; Figure 3, a to e; Figure 4 a and b). Reactive astrocytes immunoreactive against the 14-3-3 protein exhibited the most dense accumulation at the lesion edge, although they were widely distributed in demyelinating lesions and in the normal appearing white matter. A glial scar was also intensely labeled with the antibodies against β, ϵ, ζ, and η isoforms (ϵ shown in Figure 3e and the others not shown). In MS and non-MS brains, a major population of cerebral cortical neurons constitutively expressed high levels of β, γ, ζ, and η isoforms, and to a lessor degree, θ isoform, whereas they hardly showed immunoreactivity for the σ isoform, and a small population of cerebral cortical neurons in MS and non-MS brains occasionally expressed weak immunoreactivity for the ϵ isoform, although these findings varied among brains for different cases (Table 2; Figure 4, c to f; and Figure 6). Disrupted, distorted, and swollen axons found in the active demyelinating lesions of MS exhibited strong immunoreactivity against γ and ζ isoforms (γ shown in Figure 5a and the other not shown).

A very small population of reactive astrocytes in demyelinating lesions of MS, which occasionally showed a binucleated morphology, intensely expressed the σ isoform, whose expression was not detected in cultured human astrocytes (Figure 5c). A number of reactive astrocytes that appeared in the ischemic lesions of cerebral infarction expressed strong immunoreactivity against ϵ, ζ, and η isoforms (Table 2; Figure 5b), and the σ isoform was again strongly expressed in a very small number of reactive astrocytes (Figure 5d). The immunoreactivity against the η isoform was often concentrated in the nuclear region of reactive astrocytes in MS lesions (not shown) and the ischemic lesions (Figure 6; a to f). Furthermore, some GFAP$^+$ astrocytes occasionally identified in the brains of schizophrenia and neurologically normal patients expressed ϵ and σ isoforms at variable levels (Table 2; Figure 6, b and e). CD68$^+$ macrophages and microglia, with the greatest accumulation identified in the center and edge of active demyelinating lesions of MS and necrotic lesions of cerebral infarction, expressed β, ζ, and η isoforms, whereas they did not show substantial immunoreactivity against ϵ, θ, or σ isoforms (Table 2; Figure 6c). CD3$^+$ lymphocytes found in the perivascular cuffs of active MS lesions expressed variable immunoreactivities for β and ζ isoforms (not shown). A substantial

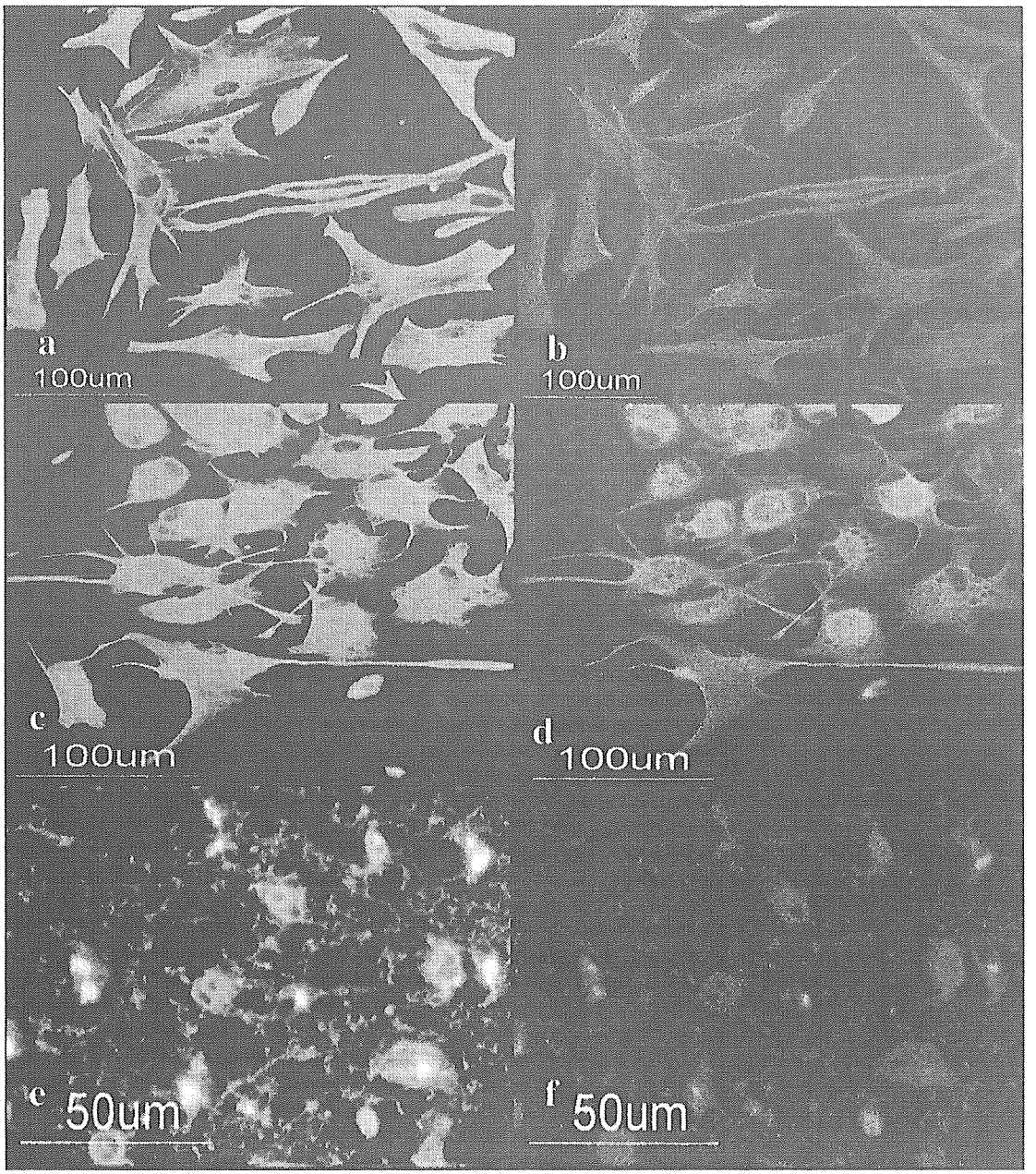

Figure 10. Co-expression of the 14-3-3 ε isoform and vimentin in cultured human astrocytes and reactive astrocytes in chronic demyelinating lesions of MS. Cultured human astrocytes and MS brain tissues were processed for double immunolabeling with anti-vimentin antibody and ε isoform-specific antibody or anti-GFAP antibody followed by labeling with fluorescein isothiocyanate- and rhodamine-conjugated secondary antibodies. **a** to **f** represent cultured human astrocytes (AS-BW) (**a–d**); no. 744, chronic active demyelinating lesions in the subcortical white matter of the frontal lobe (**e**, **f**); vimentin (**a**, **c**, **e**); ε (**b**, **f**); and GFAP (**d**).

population of oligodendrocytes, which survived in chronic active demyelinating lesions of MS and ischemic lesions of cerebral infarction, expressed intense immunoreactivity against θ isoform (Table 2; Figure 5, e and f; and Figure 6d). These results suggest that markedly up-regulated expression of the ε isoform is the most reliable marker for identifying reactive astrocytes in MS and non-MS brains. Co-expression of the ε isoform and GFAP was verified in reactive astrocytes in MS lesions (Figure 7; a to c) and cultured human astrocytes (Figure 7; d to f) by double immunolabeling.

Binding of the 14-3-3ε Isoform to Vimentin and GFAP in Cultured Human Astrocytes

To identify the binding partner of the 14-3-3 protein in human astrocytes, we performed a protein overlay anal-

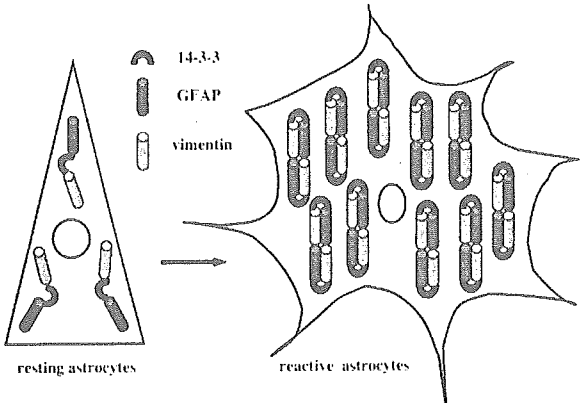

Figure 11. Putative role of the 14-3-3 protein in reactive gliosis in MS. Reactive gliosis is characterized by hypertrophy and proliferation of astrocytes associated with enhanced expression of GFAP (green) and vimentin (orange), which are co-polymerized in assembled filaments. Cultured human astrocytes expressed β, γ, ϵ, ζ, η, and θ isoforms, whose levels were markedly up-regulated under the growth-promoting culture condition, in which the 14-3-3 protein (red) interacted with vimentin (orange) and GFAP (green). These observations suggest that the 14-3-3 protein (red) might act as an adaptor that connects vimentin (orange) and GFAP (green) in reactive astrocytes at the site of demyelinating lesions in MS.

ysis using recombinant human 14-3-3ε protein with the Xpress tag (rh14-3-3ε) as a probe. Human astrocytes were incubated in 10% FBS-containing culture medium. Total protein extract was separated on a two-dimensional PAGE gel (Figure 8A, a) and transferred onto a polyvinylidene difluoride membrane (Figure 8A, b to h). The rh14-3-3ε probe strongly reacted with several spots on the blot, among which two major 54-kd spots were designated spots no. 1 and no. 2 (Figure 8A, b). In contrast, the rhISG15 probe did not react with these spots, excluding nonspecific binding of rh14-3-3ε via the Xpress tag (Figure 8A, h). Spots no. 1 and no. 2 were excised from the original gels, trypsinized, and processed for nanoESI-MS/MS analysis (Figure 9A). Among the peaks detected, eight peptide fragments derived from spot no. 1 and six from spot no. 2 showed a perfect match with the amino acid sequence covering residues 51 to 466 of human vimentin (Figure 9B), suggesting that these spots correspond to nearly full-length vimentin. Intense vimentin immunoreactivity was also identified in reactive astrocytes in demyelinating lesions of MS (Figure 3f). Furthermore, anti-vimentin monoclonal antibody reacted with spots no. 1 and no. 2, although this antibody labeled three additional, more acidic spots having smaller molecular weights (Figure 8A, c). The latter might represent post-translationally modified isoforms or degradation products of vimentin. Because vimentin is heavily phosphorylated at multiple serine residues in various mesenchymal cells, the phosphorylation state was characterized by repeated relabeling of the blot with three different antibodies specific for phosphorylated serine epitopes of vimentin. Phosphorylated Ser-39-, Ser-72-, and Ser-83-specific antibodies strongly reacted with spots no. 1 and no. 2, along with three additional spots unlabeled with rh14-3-3ε, suggesting that these serine residues are not involved in the interaction of the ε isoform with vimentin (Figure 8A, d to f). Protein overlay analysis using the rh14-3-3ε probe identified a distinct spot, designated spot no. 3 (Figure 8A, b). This spot was labeled with anti-GFAP antibody, indicating that GFAP is another binding partner of the 14-3-3 protein (Figure 8A, g). A more acidic spot having a smaller molecular weight immunoreactive for GFAP and weakly labeled with rh14-3-3ε might represent a post-translationally modified isoform or a degradation product of GFAP (Figure 8A, b and g). Vimentin and GFAP were detected in the immunoprecipitates of cultured human astrocyte protein extract, when the lysate was incubated with the ε, β, or ζ isoform-specific antibody (Figure 8B, top and bottom panels, lanes 1 to 3, 6 to 8). In contrast, only marginal bands were found in those with normal rabbit IgG (Figure 8B, top and bottom panels, lanes 4 and 9). Co-expression of the ε isoform with vimentin and GFAP was verified in cultured human astrocytes (Figure 10; a to d) and in reactive astrocytes in demyelinating lesions of MS (Figure 10, e and f) by double immunolabeling.

Discussion

The present study showed that seven 14-3-3 isoforms are differentially expressed in reactive astrocytes in demyelinating lesions of MS. Human astrocytes in culture also expressed β, γ, ε, ζ, η, and θ isoforms whose levels were markedly elevated under the growth-promoting culture condition. In demyelinating lesions of MS, the majority of GFAP$^+$ hypertrophic astrocytes intensely expressed β, ε, ζ, and η isoforms, although the expression of these isoforms was found in reactive astrocytes appearing in non-MS brains. Previous studies showed that the σ isoform expression is confined to differentiated squamous epithelial cells.[19,38] However, we found that some reactive astrocytes in MS and non-MS brains intensely expressed this isoform. Neurons constitutively expressed β, γ, ζ, and η isoforms but they did not constantly express ε or σ isoforms. Macrophages and microglia in MS and non-MS lesions intensely expressed β, ζ, and η isoforms, but they did not express ε, θ, or σ isoforms. A substantial population of oligodendrocytes, surviving in active demyelinating lesions of MS and ischemic lesions of cerebral infarction, intensely expressed the θ isoform, consistent with the expression of this isoform in the white matter of the developing rat CNS.[7] These observations are in agreement with our previous findings that the 14-3-3 protein is expressed not only in neurons but also in astrocytes, microglia, and oligodendrocytes in mouse brain cell cultures.[26] The present observations suggest that up-regulated expression of the ε isoform could be used as an immunohistochemical marker to identify reactive astrocytes at least in demyelinating lesions of MS and ischemic lesions of cerebral infarction. However, Lewy bodies in the Parkinson's disease brain[30] and a minor population of neurons in MS and non-MS brains express the ε isoform, indicating that this isoform is not astrocyte-specific.

The biological role of ε and σ isoforms in human astrocyte function remains unknown. Increasing evidence indicates that isoform-specific function regulates the devel-

opment and differentiation of neural and nonneural cells. Particularly, the ε isoform plays a role in the regulation of various cellular signaling events. The 14-3-3ε gene is deleted in the patients with Miller-Dieker syndrome, a human neuronal migration disorder presenting with the most severe form of lissencephaly (LIS) associated with facial abnormalities.[39] ε Isoform-deficient mice are defective in neuronal migration during brain development.[40] The multimolecular complex composed of the ε isoform, LIS1 and nudE nuclear distribution gene E homolog-like 1 (NUDEL) regulates the activity of dynein, a cytoplasmic motor protein, suggesting a role of ε in neuronal migration.[40] Somatic homozygous deletion of the 14-3-3ε gene is frequently found in small cell lung cancers, supporting the idea that the ε isoform serves as a tumor suppressor gene.[41] The 14-3-3ε isoform, by binding to the intracellular domain of the p75 neurotrophin receptor (NTR) in a NGF-dependent manner, promotes p75NTR-associated cell death executor (NADE)-mediated apoptosis.[42] During apoptosis, the ε protein is cleaved by caspase-3 at a cleavage site located in the C-terminal hydrophobic tail, where the amino acid sequence is highly variable among different 14-3-3 isoforms.[43] The ε isoform interacts with cdc25A and cdc25B phosphatases, key enzymes required for cell-cycle progression by activating cyclin-dependent kinases.[44] Phosphorylation-dependent interaction of the ε isoform with heat shock transcription factor HSF1 restricts the location of HSF1 in the cytoplasm by keeping it in an inactive form.[45] The ε isoform catalyzes the depolymerization and unfolding of mitochondrial precursor proteins in an ATP-dependent manner.[46] Based on these observations, we propose that the ε isoform plays a regulatory role in proliferation, apoptosis, and stress responses in reactive astrocytes.

The σ isoform constitutes a component of the G_2/M cell-cycle checkpoint machinery.[47] Exposure of the cells to DNA-damaging agents results in p53-dependent induction of the σ isoform, which in turn arrests the cells in the G_2/M phase by sequestering the cdc2-cyclin B1 complex in the cytoplasm.[48] Therefore, σ isoform-deficient cells are unable to maintain cell-cycle arrest.[47] Selective down-regulation of the σ isoform because of the hypermethylation of CpG islands in its promoter region is responsible for the malignant transformation of breast cancer cells,[49] whereas reduced expression of the σ isoform allows human epidermal keratinocytes to escape replicative senescence.[50] These observations raise the possibility that a population of reactive astrocytes with strong immunoreactivity against the σ isoform might represent the cells responding to DNA damage at the site of demyelinating lesions in MS and ischemic lesions of cerebral infarction.

Reactive gliosis is characterized by hypertrophy and proliferation of astrocytes associated with enhanced expression of GFAP and vimentin, accompanied by increased production of growth factors, cytokines, neuropeptides, and extracellular matrix molecules.[51,52] Astrocytes play a role in the repair of the blood-brain barrier, protection of neurons from glutamate excitotoxicity, and enhancement of neuronal survival by supplying neurotrophic factors.[53] On the other hand, reactive astrocytes strongly inhibit neurite outgrowth by forming glial scars after CNS injury and inflammation.[53,54] Through protein overlay and nanoESI-MS/MS analysis, we showed that vimentin is the major 14-3-3 protein-interacting protein expressed in cultured human astrocytes. Consistent with previous observations,[55,56] we identified vimentin expression in reactive astrocytes in demyelinating lesions of MS. Astrocytes isolated from vimentin-deficient mice possess an abnormal filamentous network of GFAP.[57,58] Furthermore, mice lacking vimentin and GFAP do not form proper glial scars after CNS injury, indicating that the type III IF family proteins play a pivotal role in cytoskeletal organization in astrocytes.[59]

In our study, the rh14-3-3ε probe strongly reacted with two distinct spots named no. 1 and no. 2 among five phosphovimentin-immunoreactive spots on the blot. Vimentin was immunoprecipitated with the ζ and β isoforms along with ε. These observations suggest that the interaction between vimentin and the 14-3-3 protein is not isoform-specific, and that the 14-3-3 protein-binding domain in vimentin might not include phosphorylated Ser-39, Ser-72, and Ser-83 epitopes. Protein overlay analysis identified GFAP as another binding partner of the 14-3-3ε isoform. Immunoprecipitation experiments verified the interaction between GFAP and the ε, ζ, or β isoform. However, a different spot strongly immunoreactive against GFAP but much weakly labeled with rh14-3-3ε was identified on the two-dimensional gel blot. This suggests that a substantial pool of cytoplasmic vimentin and GFAP proteins steadily interact with the 14-3-3 protein in human astrocytes.

Our observations raise the possibility that the 14-3-3 protein acts as an adaptor that connects vimentin and GFAP in cultured human astrocytes (Figure 11). Previous studies showed that vimentin and GFAP are co-expressed and co-polymerized in assembled filaments in astrocytes,[58,60] supporting the view that the 14-3-3 protein not only bridges vimentin and GFAP one by one, but also bundles both of them in the same assembled filaments. All these proteins are expressed at much higher levels in reactive astrocytes, which require more efforts to coordinate the IF network compared with resting astrocytes (Figure 11). Several other binding partner candidates for vimentin in astrocytes include α-crystallin, which inhibits the *in vitro* assembly of GFAP,[61] and the multiple endocrine neoplasia type 1 (MEN1) gene product named menin, which binds to vimentin and GFAP in glioma cells.[62] The 14-3-3γ isoform interacts with F-actin and Raf kinase in cultured mouse astrocytes, indicating its role in cytoskeletal rearrangement during cell growth and division.[63,64] Importantly, a recent study using COS-7 cells overexpressing the 14-3-3 protein showed that phosphorylated vimentin binds to the 14-3-3 protein and limits the interaction of 14-3-3 with other 14-3-3-binding partners, thereby modulating Raf-dependent intracellular signaling.[65] This study also found that vimentin does not have typical consensus 14-3-3-binding motifs.[65] However, a close interaction of the 14-3-3 protein with phosphorylated vimentin affects the phosphorylation and dephosphorylation state of vimentin.[65] Site-specific phosphorylation of vimentin and GFAP is mediated by

a range of protein kinases, including Rho kinase, cdc2 kinase, Ca^{2+} calmodulin-dependent kinase II, protein kinases A and C, and Aurora-B kinase.[60,66–69] They coordinately regulate dynamic equilibrium between the assembly and disassembly of IF proteins during mitosis.[60,66–69] Furthermore, these kinases are identified as binding partners for the 14-3-3 protein.[1–3] Therefore, our observations suggest that the 14-3-3 protein plays a role in the organization of IF proteins and IF-related kinases during conversion from resting astrocytes to reactive astrocytes. A role for 14-3-3 protein in IF dynamics is supported by our preliminary observations that suggest the effects of difopein,[70] a specific inhibitor of 14-3-3 protein/ligand interaction, on the morphological characteristics of cultured human astrocytes.

Acknowledgments

We thank Dr. Mitsuru Kawai, Department of Neurology, National Center Hospital for Mental, Nervous, and Muscular Disorders, NCNP, Tokyo, Japan, for providing information about MS patients; Dr. Toshikazu Murakami, Department of Pathology, Kohnodai Hospital, NCNP, Chiba, Japan, for providing the brains of neurologically normal controls; Drs. Kazuhiko Watabe and S.U. Kim, University of British Columbia, Vancouver, BC, Canada, for providing cultured fetal human astrocytes; and Dr. Masashi Fukuda, Invitrogen Proteome, Yokohama, Japan, for his help in nanoESI-MS/MS analysis.

References

1. Fu H, Subramanian RR, Masters SC: 14-3-3 proteins: structure, function, and regulation. Annu Rev Pharmacol Toxicol 2000, 40:617–647
2. van Hemert MJ, Steensma HY, van Heusden GPH: 14-3-3 proteins: key regulators of cell division, signaling and apoptosis. Bioessays 2001, 23:936–947
3. Aitken A, Baxter H, Dubois T, Clokie S, Mackie S, Mitchell K, Peden A, Zemlickova E: 14-3-3 proteins in cell regulation. Biochem Soc Trans 2002, 30:351–360
4. Berg D, Holzmann C, Riess O: 14-3-3 proteins in the nervous system. Nature Rev Neurosci 2002, 4:752–762
5. Boston PF, Jackson P, Kyonoch PAM; Thompson RJ: Purification, properties, and immunohistochemical localisation of human brain 14-3-3 protein. J Neurochem 1982, 38:1466–1474
6. Watanabe M, Isobe T, Ichimura T, Kuwano R, Takahashi Y, Kondo H: Molecular cloning of rat cDNAs for β and γ subtypes of 14-3-3 protein and developmental changes in expression of their mRNAs in the nervous system. Mol Brain Res 1993, 17:135–146
7. Watanabe M, Isobe T, Ichimura T, Kuwano R, Takahashi Y, Kondo H, Inoue Y: Molecular cloning of rat cDNAs for the ζ and θ subtypes of 14-3-3 protein and differential distributions of their mRNAs in the brain. Mol Brain Res 1994, 25:113–121
8. Muslin AJ, Xing H: 14-3-3 proteins: regulation of subcellular localization by molecular interference. Cell Signal 2000, 12:703–709
9. Yaffe MB: How do 14-3-3 proteins work?—gatekeeper phosphorylation and the molecular anvil hypothesis. FEBS Lett 2002, 513:53–57
10. Tzivion G, Avruch J: 14-3-3 proteins: active cofactors in cellular regulation by serine/threonine phosphorylation. J Biol Chem 2002, 277:3061–3064
11. Zhai J, Lin H, Shamim M, Schlaepfer WW, Cañete-Soler R: Identification of a novel interaction of 14-3-3 with p190RhoGEF. J Biol Chem 2001, 276:41318–41324
12. Dai J-G, Murakami K: Constitutively and autonomously active protein kinase C associated with 14-3-3 ζ in the rodent brain. J Neurochem 2003, 84:23–34
13. Broadie K, Rushton E, Skoulakis EMC, Davis RL: Leonardo, a Drosphila 14-3-3 protein involved in learning, regulates presynaptic function. Neuron 1997, 19:391–402
14. Meller N, Liu Y-C, Collins TL, Bonnefoy-Bérard N, Naier G, Isakov N, Altman A: Direct interaction between protein kinase Cθ (PKCθ) and 14-3-3τ in T cells: 14-3-3 overexpression results in inhibition of PKCθ translocation and function. Mol Cell Biol 1996, 16:5782–5791
15. Craparo A, Freund R, Gustafson TA: 14-3-3 (ϵ) interacts with the insulin-like growth factor I receptor and insulin receptor substrate I in a phosphoserine-dependent manner. J Biol Chem 1997, 272:11663–11669
16. Vincenz C, Dixit VM: 14-3-3 proteins associate with A20 in an isoform-specific manner and function both as chaperone and adaptor molecules. J Biol Chem 1996, 271:20029–20034
17. Wakui H, Wright APH, Gustafsson J-A, Zilliacus J: Interaction of the ligand-activated glucocorticoid receptor with the 14-3-3η protein. J Biol Chem 1997, 272:8153–8156
18. Hashiguchi M, Sobue K, Paudel HK: 14-3-3ζ is an effector of tau protein phosphorylation. J Biol Chem 2000, 275:25247–25254
19. Leffers H, Madsen P, Rasmussen HH, Honoré B, Andersen AH, Walbum E, Vandekerckhove J, Celis JE: Molecular cloning and expression of the transformation sensitive epithelial marker stratifin. A member of a protein family that has been involved in the protein kinase C signaling pathway. J Mol Biol 1993, 231:982–998
20. Martin H, Rostas J, Patel Y, Aitken A: Subcellular localisation of 14-3-3 isoforms in rat brain using specific antibodies. J Neurochem 1994, 63:2259–2265
21. Baxter HC, Liu W-G, Forster JL, Aitken A, Fraser JR: Immunolocalisation of 14-3-3 isoforms in normal and scrapie-infected murine brain. Neuroscience 2002, 109:5–14
22. Hsich G, Kenney K, Gibbs Jr CJ, Lee KH, Harrington MG: The 14-3-3 brain protein in cerebrospinal fluid as a marker for transmissible spongiform encephalopathies. N Engl J Med 1996, 335:924–930
23. Zerr I, Bodemer M, Gefeller O, Otto M, Poser S, Wiltfang J, Windl O, Kretzschmar HA, Weber T: Detection of 14-3-3 protein in the cerebrospinal fluid supports the diagnosis of Creutzfeldt-Jakob disease. Ann Neurol 1998, 43:32–40
24. Wiltfang J, Otto M, Baxter HC, Bodemer M, Steinacker P, Bahn E, Zerr I, Kornhuber J, Kretzschmar HA, Poser S, Rüther E, Aitken A: Isoform pattern of 14-3-3 proteins in the cerebrospinal fluid of patients with Creutzfeldt-Jakob disease. J Neurochem 1999, 73:2485–2490
25. Richard M, Biacabe A-G, Streichenberger N, Ironside JW, Mohr M, Kopp N, Perret-Liaudet A: Immunohistochemical localization of 14.3.3 ζ protein in amyloid plaques in human spongiform encephalopathies. Acta Neuropathol 2003, 105:296–302
26. Satoh J, Kurohara K, Yukitake M, Kuroda Y: The 14-3-3 protein detectable in the cerebrospinal fluid of patients with prion-unrelated neurological diseases is expressed constitutively in neurons and glial cells in culture. Eur Neurol 1999, 41:216–225
27. Satoh J, Yukitake M, Kurohara K, Takashima H, Kuroda Y: Detection of the 14-3-3 protein in the cerebrospinal fluid of Japanese multiple sclerosis patients presenting with severe myelitis. J Neurol Sci 2003, 212:11–20
28. Layfield R, Fergusson J, Aitken A, Lowe J, Landon M, Mayer RJ: Neurofibrillary tangles of Alzheimer's disease brains contain 14-3-3 proteins. Neurosci Lett 1996, 209:57–60
29. Agarwal-Mawal A, Qureshi HY, Cafferty PW, Yuan Z, Han D, Lin R, Paudel HK: 14-3-3 connects glycogen synthase kinase-3β to tau within a brain microtubule-associated tau phosphorylation complex. J Biol Chem 2003, 278:12722–12728
30. Berg D, Riess O, Bornemann A: Specification of 14-3-3 proteins in Lewy bodies. Ann Neurol 2003, 54:135
31. Ostrerova N, Petrucelli L, Farrer M, Mehta N, Choi P, Hardy J, Wolozin B: α-Synuclein shares physical and functional homology with 14-3-3 proteins. J Neurosci 1999, 19:5782–5791
32. Xu J, Kao S-Y, Lee FJS, Song W, Jin L-W, Yanker BA: Dopamine-dependent neurotoxicity of α-synuclein: a mechanism for selective neurodegeneration in Parkinson disease. Nat Med 2002, 8:600–606
33. Chen H-K, Fernandez-Funez P, Acevedo SF, Lam YC, Kaytor MD, Fernandez MH, Aitken A, Skoulakis EMC, Orr HT, Botas J, Zoghbi HY: Interaction of Akt-phosphorylated ataxin-1 with 14-3-3 mediates neurodegeneration in spinocerebellar ataxia type 1. Cell 2003, 113:457–468